ADA026 884

Unclassified

SECURITY CLASSIFICATION OF THIS PAGE (When Data Entered)

REPORT DOCUMENTATION PAGE

READ INSTRUCTIONS BEFORE COMPLETING FORM

1. REPORT NUMBER: Contract Report S-76-5
2. GOVT ACCESSION NO.:
3. RECIPIENT'S CATALOG NUMBER:

4. TITLE (and Subtitle): THE INFLUENCES OF SAND FABRIC ON LIQUEFACTION BEHAVIOR
5. TYPE OF REPORT & PERIOD COVERED: Final report
6. PERFORMING ORG. REPORT NUMBER:

7. AUTHOR(s): James K. Mitchell, John M. Chatoian, Gary C. Carpenter
8. CONTRACT OR GRANT NUMBER(s): DACA39-75-M0260

9. PERFORMING ORGANIZATION NAME AND ADDRESS: College of Engineering, University of California, Berkeley, Calif. 94720
10. PROGRAM ELEMENT, PROJECT, TASK AREA & WORK UNIT NUMBERS: Project 4A161102AT22, Task A2, Work Unit 005

11. CONTROLLING OFFICE NAME AND ADDRESS: Office, Chief of Engineers, U. S. Army, Washington, D. C. 20314
12. REPORT DATE: June 1976
13. NUMBER OF PAGES: 79

14. MONITORING AGENCY NAME & ADDRESS (if different from Controlling Office): U. S. Army Engineer Waterways Experiment Station, Soils and Pavements Laboratory, P. O. Box 631, Vicksburg, Miss. 39180
15. SECURITY CLASS. (of this report): Unclassified
15a. DECLASSIFICATION/DOWNGRADING SCHEDULE:

16. DISTRIBUTION STATEMENT (of this Report): Approved for public release; distribution unlimited.

83 p.

17. DISTRIBUTION STATEMENT (of the abstract entered in Block 20, if different from Report): RDT/E-4-A-161102-AT-22

18. SUPPLEMENTARY NOTES: 4-A-161102-AT-22-A-2

19. KEY WORDS (Continue on reverse side if necessary and identify by block number):
Liquefaction (Soils)
Sands
Soil fabric
Triaxial shear tests

WES

CR-S-76-5

20. ABSTRACT (Continue on reverse side if necessary and identify by block number):

Relationships between sand fabric, sample preparation method, and liquefaction and drained compression behavior under triaxial loading were determined for Monterey No. 0 sand. Reproducible samples were fabricated at 50 percent relative density using pluvial, moist tamping, and moist vibration methods of compaction. Pluviation and moist tamping were used to prepare samples at 80 percent relative density. Fabric was characterized by particle

(Continued)

DD FORM 1 JAN 73 1473 EDITION OF 1 NOV 65 IS OBSOLETE

Unclassified

SECURITY CLASSIFICATION OF THIS PAGE (When Data Entered)

20. ABSTRACT (Continued).

long axis and interparticle contact orientations.

Samples at both 50 percent and 80 percent relative density prepared by dry pluviation exhibited much lower strength under cyclic loading than did samples prepared by the other methods. At 50 percent relative density samples prepared by pluviation were less stiff, compressed more prior to dilation and dilated less than samples prepared by the other methods. Differences were less pronounced at 80 percent relative density.

Preferred orientation of long axes of particles developed in the horizontal direction for each of the methods studied, with the intensity increasing in the order moist vibration (nearly random), moist tamping, dry pluviation.

At a relative density of 50 percent preferred orientation of interparticle contact planes existed in the range of $\pm 0°$ to 30° of the horizontal with the proportion increasing in the order dry pluviation, moist tamping, moist vibration. At 80 percent relative density more interparticle contact plane orientations were in the range of $\pm 0°$ to 30° of the horizontal for samples prepared by dry pluviation than by moist tamping.

For a given average relative density substantial variations in density in a longitudinal direction could be seen in X-radiographs. These variations differed for sample preparation by different methods.

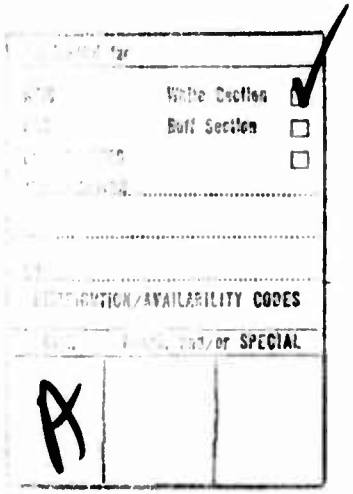

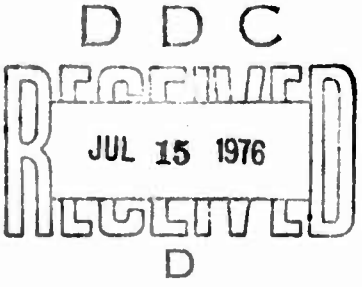

PREFACE

This report was prepared by Professor J. K. Mitchell and Messrs. J. M. Chatoian and G. C. Carpenter under Contract DACA 39-75-M0260 as part of on-going work conducted at the U. S. Army Engineer Waterways Experiment Station (WES) under the sponsorship of the Directorate of Military Construction, Office, Chief of Engineers, under Research in Military Construction, Project 4A161102AT22, Task A2, Work Unit 005, Study of Engineering Classification of Cohesionless Soils.

The work was performed under the direction of Drs. J. P. Mulilis and F. C. Townsend, Research Civil Engineers, Soil Mechanics Division, Soils and Pavements Laboratory (S&PL). General guidance was provided by the following S&PL personnel: Messrs. J. P. Sale and S. J. Johnson, Chief and Special Assistant, respectively, S&PL; and Mr. C. L. McAnear, Chief, Soil Mechanics Division.

Director of WES during this study and preparation and publication of this report was COL G. H. Hilt, CE. Technical Director was Mr. F. R. Brown.

CONVERSION FACTORS, U. S. CUSTOMARY TO METRIC (SI)
UNITS OF MEASUREMENT

Multiply	By	To Obtain
inches	25.4	millimetres
inches of mercury ($60^{\circ}F$)	3376.85	pascals
feet	0.3048	metres
pounds (mass)	0.4535924	kilograms
pounds (force)	4.448222	newtons
pounds (force) per square inch	6894.757	pascals
pounds (mass) per cubic foot	16.01846	kilograms per cubic metre
cycles per second	1.0	Hertz

CONTENTS

LIST OF FIGURES

LIST OF TABLES

I. INTRODUCTION

In recent studies (Ladd, 1974; Mulilis et al, 1975) it was found that the method of sample preparation had a significant influence on the liquefaction behavior of sands under cyclic loading. Figure 1 shows the relationship between cyclic deviator stress in undrained triaxial tests as a function of number of cycles to cause initial liquefaction. Initial liquefaction is defined as the condition when the pore pressure has increased to a value equal to the confining pressure.

Differences in strength under cyclic loading of the magnitude shown in Fig. 1 have important implications in engineering practice if reconstituted samples of sand are to be used for evaluation of strengths of sand deposits or sand fills in the field. In view of the difficulty of obtaining undisturbed samples of sand from the field and the uncertainty as to how undisturbed "undisturbed samples" really are, it is nonetheless desirable to use reconstituted samples if possible.

One approach to the selection of an appropriate laboratory sample preparation procedure is to study the fabric of the particulate sand structure formed by different methods in conjunction with the observed differences in liquefaction behavior. Then, if the fabrics of field samples can be evaluated, the reconstitution of samples with appropriate fabric in the laboratory should be possible. With the exception of the results of studies by sedimentologists of long axis orientations, fabric details of sands in the field remain largely undetermined at the present time. Their determination should be relatively easy. In addition studies of sand fabric are useful to provide a better understanding of the basic factors controlling the engineering properties of soils.

Previous work by Oda (1972), Mahmood (1973), and Mahmood and Mitchell (1974) has established that the static strength and compressibility behavior

of sands and silts depends on the fabric. In an investigation reported by Mulilis et al (1975) it was shown that the fabrics of samples of Monterey No. 0 sand prepared by two different methods, dry pluviation and moist tamping, were different, as were also the undrained strengths in undrained cyclic triaxial tests. Of interest in their study were the orientations of particle long axes and interparticle contact planes. Their results were limited, however, in that insufficient data were obtained to obtain a complete distribution of contact orientations, and only one relative density was studied. Thus the conclusions concerning fabric effects were necessarily tentative.

The purposes of the present study were to make a more in-depth study of the fabric of sand samples in relation to method of compaction and to relate these fabrics to strengths under cyclic loading. In addition behavior in drained triaxial compression was also studied, because it was considered that the stress-strain and volume change-strain characteristics should relate to both the fabric and the liquefaction behavior.

All testing was done using Monterey No. 0 sand, with samples prepared to relative densities of 50 percent and 80 percent. Only the behavior at a relative density of 50 percent was studied by Mulilis et al. Emphasis in the fabric study was on grain and interparticle contact orientations, as previous work by Oda (1972a, 1972b) had indicated them to be of particular significance.

II. SAMPLE PREPARATION

Introduction

In the previous study by Mulilis et al (1975) it was found that for Monterey No. 0 sand at a relative density of 50 percent the greatest differences in strength under cyclic loading were between samples prepared by dry pluviation and moist vibration, as shown in Fig. 1. Thus these methods were adopted for this investigation. In addition it was desired to compare cyclic strengths and fabrics of samples of the same sand at a relative density of 80 percent. As samples could not be prepared to this higher relative density using moist vibration, a moist tamping procedure was used. Samples were also prepared at a relative density of 50 percent by moist tamping for comparative purposes. Cylindrical samples prepared by all methods were approximately 2.8 inches in diameter and 7.0 inches high. A split mold lined with an impervious rubber membrane was used.

The testing program, therefore, encompassed relative densities and compaction methods as follows:

	Relative Density	
Compaction Method	50%	80%
Dry Pluviation	X	X
Moist Vibration	X	
Moist Tamping	X	X

Sand Properties

All tests were done using Monterey No. 0 sand, a uniform medium sand with rounded to subrounded grains consisting predominantly of quartz with some feldspar and mica. The maximum and minimum dry densities of

this sand are 105.7 pcf and 89.3 pcf, respectively. A grain size distribution curve is shown in Fig. 2 and a grain shape histogram of particle length to width ratios is shown in Fig. 3.

Pluvial Compaction

Dry sand was poured from a 1000 ml flask through a one-hole rubber stopper containing a nozzle of either 0.27 inch, 0.20 inch, or 0.15 inch diameter. Sand free fall to the surface of the sample was about 7 inches. The relative density obtained was a function of the intensity of particle rain, which, in turn, depended on nozzle size and rate of flask rotation above the sample as follows:

a. Decreased nozzle diameter resulted in increased relative density.

b. Increased flask rotation rate resulted in increased relative density.

Compaction by Horizontal High Frequency Vibrations

The sand was uniformly mixed to an initial moisture content of 8 percent. Samples were fabricated in seven one-inch thick layers, each vibrated under a uniform surcharge pressure of 0.8 psi. Circumferential vibrations were applied to the outside of the mold using a BVI Vibro-Graver at a frequency of 120 cps.

To prevent overdensification of the lower layers during vibration of the upper layers the "undercompaction" procedure described by Mulilis et al (1975) was used. The initial as-compacted relative densities of each one-inch layer to give a final uniform relative density of 50 percent were:

Layer No. (from bottom up)	Relative Density (%)
1	47
2	48
3	49
4	50
5	51
6	52
7	53

The surface of each layer was scarified prior to placement of the next layer. The sample mixing container and mold were filled with CO_2 initially to facilitate subsequent saturation for drained triaxial and cyclic load testing.

Compaction by Moist Tamping

The hand tamper and procedure described by Mulilis et al (1975), Fig. 4-2 and p. 57, were used. The samples were prepared in seven one-inch thick layers. For samples at 50 percent relative density the same undercompaction was used as for samples prepared by moist vibration. To obtain uniform samples at a relative density of 80 percent the following initial layer relative densities were used:

Layer No. (from bottom up)	Relative Density (%)
1	77
2	78
3	79
4	80
5	81
6	82
7	83

The top surface of each layer was scarified prior to placement of the next layer.

Resin Impregnation

Moist samples were first dried in a forced air oven at 60°C. Warm air was drawn slowly through the sample by connecting the bottom of the sample mold to a vacuum of about 1 psi and allowing warm air to enter through the top. From two to five hours were required to complete the drying process.

The sample to be impregnated was then cooled and subjected to a vacuum of 5 to 7 psi. Koppers polyester resin No. 1086-4, mixed with 20 percent (by volume) styrene (Koppers No. VM-901) to reduce viscosity and 1 percent (by volume) organic peroxide (Witco Chemical HI-Point-180) as catalyst, was introduced at the bottom of the sample. After saturation the sample was left undisturbed until initial set of the resin had occurred. The sample was then removed from the mold and placed in a forced air oven at 60°C for 24 hours to permit the resin to cure.

Four impregnated samples were prepared for each relative density and compaction method, for a total of 20 samples.

Thin Sections

Three thin sections were cut from the central portions of three of the four impregnated samples at orientations as shown in Fig. 4. By determining grain and contact orientations in each of these thin sections, the distributions in all directions within the sample could be determined. This was not possible in the preliminary fabric study described in Mulilis et al (1975).

Petrographic thin sections, about 60 μm thick, 20 mm wide, and 30 mm long, were prepared using standard methods.

Photomicrographs of typical thin sections of samples prepared by each of the methods and relative densities used in this study are shown in Figs. 5 through 9. Vertical thin sections (sections parallel to cylindrical sample axis) are shown in each case.

X-Radiographs

Longitudinal slices about 3 mm thick were cut from the remaining cylindrical sample of each set of four. Transmission X-radiographs were obtained using a medical X-ray machine. X-radiographs for samples prepared to a relative density of 50 percent are shown in Fig. 10, and to a relative density of 80 percent in Fig. 11.

III. FABRIC ANALYSIS

Fabric elements studied quantitatively were the three-dimensional distributions of normals to interparticle contact planes and the orientations of apparent long axes in the plane of the thin section. Other fabric elements that may have an important influence on the cyclic load strength and other mechanical properties, such as pore sizes and pore size distributions, particle clustering, if any, void variability within samples, and particle size segregation, could not be investigated within the limits of time and resources available for this study.

Universal Stage Microscope

A microscope equipped with a universal stage was used to determine particle and contact orientations. The universal stage, shown schematically in Fig. 12, allows independent rotation of the thin section about three orthogonal reference axes. The thin section is covered by the upper glass hemisphere, H in Fig. 12, set in the metal mount M. The thin section is aligned and moved with the aid of the sledge R which moves vertically in a slot cut in the hemisphere mount. Rotation can be made about the NS, EW, and vertical axes, and the amount of rotation is measured on the appropriate vernier.

The use of the universal stage microscope is described in detail by Turner and Weiss (1963).

Sampling Methods

The long axis orientations and contact plane orientations can be considered as two-dimensional sample populations because the thickness of the thin sections is very small compared to their length and width. Several methods of sampling two-dimensional populations are available (Koch and Link, 1970; Miller and Kahn, 1962; Kellerhals and Bray, 1971; Pincus, 1953):

1. Sample the entire population.

This is the only method that can describe the true orientation of the entire population. This method is impractical for very large populations, as is the case here.

2. Grid sampling.

A grid is established over the sample and only those grains or contacts immediately below the grid points are counted. A variation of this method is to assign a number to each grid block and to count entire populations within randomly selected grid blocks.

3. Transect sampling.

Every member of the parent population that falls under a straight line or narrow strip across the sample is counted.

4. Random sampling.

Randomly chosen members of the parent population are measured. This method is the most susceptible to sampling bias.

The transect sampling method was used in this investigation, because (1) the population was too large to sample in its entirety, (2) no grid attachment was available for the microscope and (3) it was necessary to avoid sampling bias. Traverses about eight or nine grains wide and about one inch long were chosen parallel to the long axis of the thin sections. Every grain or contact within this zone was counted.

Apparent Longest Axis Orientations

The orientation of a particle is represented by the inclination of its true long or short axis with respect to fixed reference axes. Determining the true orientation of the long or short axis of small particles is difficult. In practice it is usually done by analyzing the orientation of apparent longest axes as seen in thin-sections. The three-dimensional

orientation of grains can be estimated from the orientations observed in sections cut in different directions.

In this study the orientations of apparent longest axes were determined in two vertical and one horizontal section for each sample. Orientations were determined for about 220 grains in each thin section by measuring the angle θ_i between the apparent longest axes and reference axis parallel to the long axis of the thin-section (Figure 4). Both percent frequency histograms (Figures 20 and 21) and rose diagrams (Figures 22 and 23) were constructed from the data thus obtained using an azimuth class interval of $\theta = 10°$ to show the concentrations of long axes in different directions.

Statistical analyses of the data were done using a vector method and test of significance presented by Curry (1956). With this method each long axis observation is considered a vector in the measured direction of unit magnitude. No distinction is made of one end of the particle from the other. All measurements are therefore made in the range $0° \leq \theta \leq 180°$, with $\theta = 0°, 180°$ corresponding to particle axes parallel to the longitudinal axis of the cylindrical sample.

A resultant vector calculated on the 180° distribution may not reflect the true central tendency of the distribution. To illustrate this point consider the following example: if the 180° range lies in the eastern semicircle, the distribution has no west components at all. North components would tend to cancel south components so the resultant vector would always possess a strong easterly central tendency even if the true central tendency lay close to the north-south line. To remedy this the angles of the observation vectors are doubled before computing the components, thus obtaining a nonsymmetric periodic distribution.

The calculations are:

$$\text{N-S component} = \Sigma n \cos 2\theta$$

$$\text{E-W component} = \Sigma n \sin 2\theta$$

where n = number of observations oriented at θ.

$$\tan 2\bar{\theta} = \frac{\Sigma n \sin 2\theta}{\Sigma n \cos 2\theta} \tag{1}$$

$$r = \sqrt{(\Sigma n \sin 2\theta)^2 + (\Sigma n \cos 2\theta)^2} \tag{2}$$

vector magnitude,

$$L = \frac{r}{\Sigma n} \times 100\% \tag{3}$$

vector direction,

$$\bar{\theta} = \frac{1}{2} \arctan \frac{\Sigma n \sin 2\theta}{\Sigma n \cos 2\theta} \tag{4}$$

The vector direction is a measure of the preferred orientation direction of long axes of sand grains. It has the advantage of being independent of the choice of origin (Curry, 1956).

The vector magnitude varies from 0 percent to 100 percent. A random (i.e.: uniform) distribution of orientations will give a vector magnitude of 0 percent. A vector magnitude of 100 percent means that all orientations are exactly the same or, in the case of grouped data, all orientations lie within the same class interval. According to Curry (1956) L is a sensitive measure of dispersion and is comparable to standard deviation but has the advantage of being independent of the choice of origin.

Curry (1956) also adapted the vector magnitude, L, for use in the Rayleigh test of significance. Rayleigh's equation is:

$$p = e^{-r^2/n} \tag{5}$$

where p = probability of obtaining a greater amplitude by pure chance combinations of random phases,

r = resultant amplitude obtained,

n = number of observations,

e = base of natural logarithms.

For the resultant amplitude, r expressed in terms of the vector magnitude,

$$r = \frac{Ln}{100} \tag{6}$$

then

$$p = e^{(-L^2 n \times 10^{-4})} \tag{7}$$

Any level of significance, p can be used. In practice the 0.05 level is commonly used for the study of sand-grain orientations. The 0.05 level means that there are only 5 chances in 100 of the determined distribution being due to chance.

It was assumed that to establish randomness there should be a minimum of 10 observations per 10° azimuth class interval. There were 18 azimuthal intervals thereby giving a minimum sample of 180 observations. After 180-200 grains were sampled for a thin section the data were tabulated and L, $\overline{\theta}$, and p determined. If the significance level was less than 0.05 (i.e.: $p > 0.05$) additional observations were made until $p < 0.05$.

One test was conducted to determine the effect of sample size using the same thin section. Two groups of data were obtained, one consisting of 198 observations and the other of 484 observations. The determined distributions were very similar, and the mean vector directions, $\overline{\theta}$, were only 10° apart. This is considered to be close agreement as any one observation is only accurate to ±2° to 4°, depending upon the grain shape. Both tests gave Rayleigh levels of significances greater than 0.05. It was therefore concluded that a sample consisting of about 200 observations would provide as accurate a measure of long axis orientation distribution as one consisting of over 450 observations, so long as $p \leq 0.05$.

Interparticle Contact Orientations

The orientation of any interparticle contact can be represented by the normals, N_i^1, N_i^2, to the tangent plane, as shown in Fig. 13. A method for analyzing the orientations of contact plane normals has been developed by Oda (1972) and was used also for this investigation.

It is convenient to express vector orientations in terms of spherical coordinates. Spherical and Cartesian coordinates are related according to

$$x = r \sin \beta \cos \alpha \tag{8a}$$

$$y = r \sin \beta \sin \alpha \tag{8b}$$

$$z = r \cos \beta \tag{8c}$$

where r is radius or vector length, and angles α and β describe vector direction (Fig. 13).

An element dA of the surface area of a sphere is given by

$$dA_{\alpha,\beta} = rd\beta \cdot r \sin\beta \, d\alpha = r^2 \sin\beta \, d\alpha d\beta \tag{9}$$

for a sphere of unit radius

$$dA_{\alpha,\beta} = \sin\beta \, d\alpha d\beta \tag{10}$$

Integration yields

$$A = \int_{\alpha} \int_{\beta} \sin\beta \, d\alpha \, d\beta \tag{11}$$

Consider M contacts within an assemblage of granular particles. At each interparticle contact there are two contact surfaces, one belonging to grain 1 and the other to grain 2. Normal directions N_i^1 and N_i^2, Figure 13, are perpendicular to the tangent plane at the contact point. The direction of N_i^2 is described by angles α and β; whereas, the direction of N_i^1 is described by $\alpha+\pi$ and $\pi-\beta$.

The distribution of interparticle contact normals can be shown by plotting their piercing points on the sphere or its graphical equivalent, the equal area stereonet (Turner and Weiss, 1963). The total number of plotted points is 2M, twice the number of contacts.

The total number of contact normals within the angular ranges $\alpha+d\alpha$ and $\beta+d\beta$ is

$$2M\, E(\alpha,\beta)\, \sin\beta\, d\alpha d\beta \tag{12}$$

where $E(\alpha,\beta)$ is the probability density of points of contact within the angular intervals, a function of both α and β. All plotted points will be included if (12) is integrated over $\alpha = 0°$ to $360°$ and $\beta = 0°$ to $180°$. Thus $E(\alpha,\beta)$ must satisfy

$$\int_\alpha \int_\beta E(\alpha,\beta)\, \sin\beta\, d\alpha d\beta = 1 \tag{13}$$

In the present investigation $E(\alpha,\beta)$ is independent of α because of the axisymmetric character of the samples studied. Thus equation (13) becomes

$$2\pi \int_\beta E(\beta)\, \sin\beta\, d\beta = 1 \tag{14}$$

As vectors N_i^1 and N_i^2 are colinear $E(\beta)$ equals $E(\pi-\beta)$. For example, the probability density in the region $\beta = 0°$ to $\beta = 10°$ is the same as in the region $\beta = 180°$ to $\beta = 170°$. As a result only the vector orientations in one hemisphere need be measured and plotted and the results doubled to obtain the density distribution over the entire sphere. Thus equation (14) becomes

$$2\left[2\pi \int_{0°}^{90°} E(\beta)\, \sin\beta\, d\beta\right] = 1 \tag{15}$$

or

$$M = 4\pi M \left[\int_{0°}^{10°} E(\beta)\, \sin\beta d\beta + \text{-----+} \int_{80°}^{90°} E(\beta)\, \sin\beta\, d\beta\right] \tag{16}$$

If M_1 is the total number of normals in the range $\beta = 0°$ to $\beta = 10°$, then

$$M_1 = 4\pi M \int_{0°}^{10°} E(\beta) \sin\beta d\beta \qquad (17)$$

Integration gives the mean value of $E_1(\beta)$ within the range $0° \leq \beta \leq 10°$,

$$E_1(\beta) = \frac{M_1}{4\pi M(\cos 0° \cos 10°)} \qquad (18)$$

Mean values of $E(\beta)$ for other intervals are calculated in a similar manner.

For an isotropic fabric $E_i(\beta)$ = constant = $\frac{1}{4\pi}$. Values of $E_i(\beta) > \frac{1}{4\pi}$ mean a greater than average proportion of contact normals at inclination β_i; whereas $E_i(\beta) < \frac{1}{4\pi}$ indicates a less than average proportion of contact normals at inclination β_i.

IV. LIQUEFACTION BEHAVIOR

Cyclic triaxial tests were done following the procedures used by Mulilis et al (1975). The purpose of these tests on samples prepared to a relative density of 50 percent was to confirm that our sample preparation techniques gave results comparable to those of Mulilis et al. If so, then it seemed reasonable that the fabric measurements and drained triaxial test results could be applied to the findings of the earlier study as well. Several tests were done by each method, and the results agreed with the curves shown in Fig. 14.

Additional cyclic load triaxial tests were done on samples at a relative density of 80 percent. The results are shown in Fig. 15. It may be seen that even at this high relative density samples prepared by moist tamping are much stronger than samples prepared by dry pluviation. It is also apparent that nozzle size for preparation of samples by dry pluviation has a consistent and significant effect, with the use of the smaller diameter nozzle (0.20 inch) giving stronger samples.

V. DRAINED TRIAXIAL COMPRESSION BEHAVIOR

Constant rate of strain drained triaxial compression tests were done on saturated samples prepared at 50 percent and 80 percent relative density by the different methods. The purpose of these tests was to determine if consistent relationships existed between the static stress-strain and volume change behavior, the fabric, and the liquefaction behavior.

After compaction the air in the voids of the samples was replaced by CO_2 to facilitate saturation. A back pressure of about 30 psi was required to attain essentially complete saturation ($B > 0.94$). All samples were equilibrated under an effective isotropic confining pressure σ'_c of 8 psi. Drained triaxial compression was carried out using an arbitrarily selected constant rate of axial deformation of 0.16 mm/min. This corresponded to about 0.09 percent axial strain per minute. Volume changes were measured to the nearest 0.01 cc.

Behavior at 50 Percent Relative Density

Deviator stress vs. axial strain and volumetric strain vs. axial strain for each of two tests on samples at 50 percent relative density prepared by dry pluviation, moist tamping and moist vibration are shown in Fig. 16. Averaged curves for the two tests by each method are shown in Fig. 17.

It may be seen that the stiffness at low strains, as indicated by the slopes of the stress-strain curves, increases in the order pluviated < moist tamped < moist vibrated. Also the amount of volumetric compression preceding dilation increases in the order moist vibrated < moist tamped < pluviated. Both of these findings are consistent with the differences in

undrained strength in cyclic loading shown in Fig. 14. The lower the modulus and the higher the tendency for volumetric compression, the greater the rate of stress transfer to the pore water under undrained conditions, and therefore the fewer cycles of loading needed to cause failure.

That different methods of sample preparation result in different sand fabrics and differences in the stress-strain and volume change strain behavior has been well established in previous studies; e.g., Oda (1972), Arthur and Menzies (1972, Mahmood (1973), Mahmood and Mitchell (1974).

From Fig. 14 it may be seen that cyclic stress ratios $\sigma_{cd}/2\sigma_o'$ required to cause liquefaction after 10 to 100 cycles range from about 0.3 to 0.5. For the value of $\sigma_o' = 8$ psi (55.2 kN/m^2) used in these tests the corresponding cyclic deviator stress is ±4.8 to 8 psi (33 to 55 kN/m^2). Fig. 17 shows that the stiffnesses and volume changes associated with drained uniaxial compression under stresses of these magnitudes are essentially the same for all three compaction methods. Thus for the first application of $+\sigma_{cd}$ in a cyclic load test there should be essentially no difference in behavior for the different samples.

It is at higher values of deviator stress that the curves begin to diverge in the drained tests. In the undrained cyclic load tests the divergence must begin with the stress reversal ($-\sigma_{cd}$). In this phase the cell pressure becomes σ_1 and the axial stress is σ_3, causing a reversal in shear stress direction. Thus the uniaxial compression and cyclic load tests are no longer strictly comparable. Nonetheless, a distinct correlation between the stiffness and volume change characteristics in drained compression and resistance to cyclic loading is evident for samples at 50 percent relative density.

Behavior at 80 Percent Relative Density

Stress vs. strain and volume change vs. strain data for samples prepared to a relative density of 80 percent by dry pluviation and moist tamping are shown in Fig. 18. Although the peak strength and the dilation are greater for the moist tamped samples, the tangent moduli for stresses up to about 50 percent of the strength and the volumetric compressions prior to dilation are essentially the same for samples prepared by both methods.

By analogy with the results at 50 percent relative density (Figs. 14, 16, and 17) it might be anticipated that differences in cyclic load strength for the samples at 80 percent relative density would be relatively small. Fig. 15 shows that this is not the case.

Differences in drained compression behavior were observed for samples prepared by pluvial compaction using different nozzle sizes, as may be seen in Fig. 19. Although the undrained cyclic loading strength was also influenced by nozzle size, Fig. 15, the differences were nowhere near as great as between the pluviation and moist tamping compaction methods.

Thus at high relative density the strength under cyclic loading does not appear to be as distinctly related to the drained triaxial compression behavior as it does at low relative density. This is illustrated further by the data in Table 1 which compare values of maximum compressive volumetric strain preceding dilation and secant modulus at 1 percent axial strain.

Table 1

Effect of Sample Preparation Method on Volume Change and Stiffness of Monterey No. 0 Sand in Undrained Triaxial Compression

Test No.	Relative Density (%)	Preparation Method	Maximum Compressive Volumetric Strain (%)[3]	Secant Modulus at 1% Axial Strain (kN/m^2)
3, 4	50.0	Pluviation[1]	0.105	140
6, 8	50.3	Moist Tamping	0.051	192
9, 10	50.0	Moist Vibration	0.044	210
11, 12	79.8	Moist Tamping	0.050	246
15, 16	80.3	Pluviation[1]	0.049	207
5, 7	79.7	Pluviation[2]	0.036	232

[1]0.27" Dia. Nozzle

[2]0.15" Dia. Nozzle

[3]Preceding Dilation

Values are the average of two tests

σ'_3 = 8 psi (55.2 kN/m^2) for all tests

VI. APPARENT LONG AXIS ORIENTATIONS

The distributions of apparent long axis orientations as seen in the thin sections and the directions and intensities (vector length, L) of preferred orientations were determined using the procedures previously described. The longitudinal axis (vertical axis) of the original cylindrical sample was used as the reference axis, for the vertical sections and long axis orientations are expressed in terms of θ, the angle between the reference axis and the long axis. Thus a value of $\theta = 0°, 180°$ means particles are oriented in a vertical direction; whereas, $\theta = 90°, 270°$ indicates horizontal (radial) orientation.

The choice of x and y axes for referencing of long axes in the horizontal sections was arbitrary. Because of radial symmetry preferred orientations in horizontal thin sections should be small and reflect only local inhomogeneities caused by uncontrollable variations during sample preparation. This expectation of randomness is borne out by the test results in Table 2 which list for each horizontal section the magnitude of preferred orientation vector L and its direction $\overline{\theta}$. It may be seen that in most cases L is small, and there is no predominant direction for $\overline{\theta}$ associated with any of the sample preparation methods.

Results for the vertical sections are listed in Table 3. It may be seen that the differences among the values for the six thin sections studied for each relative density and compaction method are small. Thus any one of the sample preparation methods used would appear to produce reasonably reproducible samples. Average values for the orientation intensity vector L and the orientation direction are given in Table 4.

Frequency histograms and orientation rose diagrams, both based on 10° azimuth class intervals, were prepared from the data for each thin section.

Table 2

Long Axis Orientations of Sand Particles in Horizontal Thin Sections

Compaction Method	Nominal Relative Density (%)	Sample Number	Number of Observations n	Vector Length L (%)	Vector Direction* $\bar{\theta}$ (°)
Pluviation	50	P1H	234	2.5	54
		P2H	216	2.8	83
		P3H	234	1.9	133
	80	P4H	240	14.1	24
		P5H	234	3.0	124
		P6H	234	7.0	37
Moist Tamped	50	MT1H	240	12.1	7
		MT2H	234	6.8	135
		MT3H	216	8.9	104
	80	MT4H	240	3.8	74
		MT5H	216	4.3	36
		MT6H	216	4.4	114
Moist Vibrated	50	MV1H	240	3.8	23
		MV2H	234	3.6	91
		MV3H	240	2.2	121

*Y-Y direction in Fig. 4 represents $\theta = 0°$.

Table 3

Long Axis Orientations of Sand Particles in Vertical Thin Sections

Compaction Method	Nominal Relative Density (%)	Sample Number	Number of Observations n	Vector Length L (%)	Vector Direction* $\bar{\theta}$ (%)
Pluviation	50	P1V1	286	18.3	86
		P1V2	234	13.5	85
		P2V1	234	19.2	87
		P2V2	234	21.5	97
		P3V1	240	19.3	86
		P3V2	216	16.7	95
	80	P4V1	240	28.5	99
		P4V2	234	38.2	77
		P5V1	240	31.9	101
		P5V2	240	28.2	76
		P6V1	216	31.2	101
		P6V2	234	36.6	80
Moist Tamped	50	MT1V1	234	18.5	86
		MT1V2	216	18.7	101
		MT2V1	234	14.9	84
		MT2V2	234	17.3	101
		MT3V1	234	19.5	83
		MT3V2	234	18.5	90

Table 3 (Cont.)

Compaction Method	Nominal Relative Density (%)	Sample Number	Number of Observations n	Vector Length L (%)	Vector Direction* $\bar{\theta}$ (%)
Moist Tamped	80	MT4V1	234	12.5	86
		MT4V2	216	15.8	78
		MT5V1	216	16.3	84
		MT5V2	216	13.0	76
		MT6V1	234	12.2	82
		MT6V2	234	12.4	100
Moist Vibrated	50	MV1V1	234	10.2	78
		MV1V2	240	13.2	105
		MV2V1	234	11.2	71
		MV2V2	240	11.1	106
		MV3V1	234	11.4	77
		MV3V2	240	13.4	100

*Z-Z direction in Fig. 4 represents $\theta = 0°$.

Table 4

Summary of Long Axis Orientation Data
Monterey No. 0 Sand

Two Vertical Thin Sections as Shown in Fig. 4 from Three Samples Prepared by Each Method. Between 216 and 286 Observations per Thin Section.

Compaction Method	Relative Density (%)	Vector Length L (%)	Vector Direction (θ)
Pluviation	50	18.1	89.3
	80	32.4	89.0
Moist Tamped	50	17.9	90.8
	80	13.7	84.3
Moist Vibrated	50	11.8	89.5

Only typical examples are shown here, corresponding to the different relative densities and compaction methods. Figs. 20 and 21 are histograms which compare samples prepared by different methods to relative densities of 50 percent and 80 percent, respectively. The horizontal dashed line in each figure represents a completely random orientation. The rose diagrams in Figures 22 and 23 are similar comparisons. The light circles shown in these figures represent a random orientation.

The vector magnitudes for samples prepared by moist tamping at 80 percent relative density and by moist vibration at 50 percent relative density, Tables 3 and 4, are small and are close to the lower level of significance according to the Rayleigh test described previously. On the other hand the vector magnitudes and sample populations for the other thin sections give a high level of significance. This is evidence that the moist tamped samples at 80 percent relative density and the moist vibrated samples at 50 percent relative density have a nearly random distribution of long axis orientations. These were the strongest samples in both undrained cyclic triaxial loading and drained triaxial compression.

Definite preferred orientation of long axes in a direction normal to the longitudinal axis was developed by pluviation. Significant orientation in the same direction was also obtained by moist tamping to a relative density of 50 percent.

Thus, for this sand and for the three methods of compaction used, it appears that for a given relative density the greater the intensity of preferred long axis orientation in a direction normal to the direction of the applied cyclic deviator stress, the less the resistance to liquefaction under triaxial loading conditions.

VII. INTERPARTICLE CONTACT ORIENTATIONS

Interparticle contact orientations, expressed in terms of the normal to the interparticle contact plane both by equal area stereonets and by the density function $E(\beta)$, developed in a previous section, were determined for each fabric and relative density combination studied. As was the case for the distribution of long axis orientations, the distributions of interparticle contact normals were remarkably similar for the three samples prepared by each method. This provides further support for the concept that different reproducible fabrics are formed by the different compaction methods.

The equal area stereonets are shown in Figs. 24 through 28. On these diagrams blank areas indicate contact normal directions within which less than one percent of the normals intersect one percent of the surface area of a sphere containing all the possible directions. Light stippled areas enclose 1 to 2 percent of the contact normals per one percent of the circumscribing sphere. The heavy stippled areas indicate more than 2 percent of the normals per one percent of the sphere surface. Thus the darker the area the greater the concentration of interparticle contact normals.

The distribution functions $E(\beta)$ for samples prepared by pluvial compaction to relative densities of 50 percent and 80 percent are compared in Fig. 29. Similar plots for samples prepared by moist tamping are shown in Fig. 30. The results for a sample prepared by moist vibration to a relative density of 50 percent are shown in Fig. 31. In these figures the light horizontal dashed line indicates the $E(\beta)$ distribution for a completely random distribution.

$E(\beta)$ distributions for samples prepared to a relative density of 50 percent by three methods are compared in Fig. 32. A comparison of two methods at a relative density of 80 percent is given in Fig. 33.

The stereonets for samples prepared by pluviation, Figs. 24 and 27, and the corresponding $E(\beta)$ distributions, Fig. 29, show that interparticle contacts are relatively randomly oriented at 50 percent relative density. At 80 percent relative density, however, there is a predominance of interparticle contact normals oriented at 0° to 30° of the vertical. This corresponds to a significant increase in the proportion of contact planes oriented at 0 to 30° to the horizontal.

Both moist tamping, Figs. 25 and 30, and moist vibration, Figs. 26 and 31, show concentrations of interparticle normals oriented in the range of 0 to 40° of the vertical for samples at 50 percent relative density, indicating preferred orientation of contact planes at 0 to 40° with the horizontal. A similar relationship is seen for samples prepared by moist tamping at a relative density of 80 percent, Figs. 28 and 30.

Comparison of the $E(\beta)$ distributions for the three compaction methods and samples at 50 percent relative density, Fig. 32, shows that the proportion of contact planes oriented in the range of 0° to 30° with the horizontal increases in the order pluviation, moist tamping, moist vibration. This is the same order of strength increase under cyclic loading. It agrees also with the order of stiffness increase and dilation in drained triaxial compression. It appears, therefore, that the greater the proportion of interparticle contacts oriented normal to the direction of the major principal stress in triaxial compression the greater the resistance to deformation and liquefaction of Monterey No. 0 sand at a relative density of 50 percent.

At 80 percent relative density samples prepared by pluviation have a somewhat greater proportion of interparticle contacts oriented close to the horizontal (0 to 30°), Fig. 33, than do samples prepared by moist tamping. This result was somewhat surprising in view of the very much higher strength under cyclic loading for the sample prepared by moist tamping, Fig. 15. The differences in strength and volume change behavior in drained triaxial compression, Fig. 18, were relatively small by comparison, but they were also in a contrary direction to the strength-contact orientation relationship found at 50 percent relative density for the pluviation and moist tamping methods.

VIII. SAMPLE UNIFORMITY

The uniformity of samples on a macroscale is revealed by the X-radiographs of vertical slices shown in Fig. 10 for a relative density of 50 percent and Fig. 11 for a relative density of 80 percent. Both moist tamping and moist vibration produce narrow (~1 mm) bands of high density at the layer boundaries. The difference between the density in this band and the remainder of each 1 inch layer at 50 percent relative density is greater than at 80 percent relative density, as may be seen by comparing the X-radiographs for moist tamped samples in Figs. 10 and 11. The banding is more intense in moist vibrated samples than in moist tamped samples, Fig. 10.

Thin (1-2 mm), wavy layers of alternating high and low density are observed in samples prepared by pluviation. Differences in these layers are less at 80 percent relative density than at 50 percent relative density. Macroscale fabric differences at 80 percent relative density resulting from pluvial and tamping compaction methods are less pronounced than at 50 percent relative density, even though the cyclic load strength differences are large at 80 percent relative density.

In a previous study (Mulilis et al, 1975) it was shown that the inclusion of layers of differing density within a sample could not be the complete cause of measured differences in the liquefaction behavior of samples prepared to the same average relative density by different methods. Nonetheless, differences of the type shown in Figs. 10 and 11 can be expected to influence the mechanical properties. The full magnitude of this influence can only be established after further study.

It seems reasonable to conclude also that moist tamping and moist vibration cannot reasonably be expected to produce macro-fabrics that

correspond to water or wind sedimented sand deposits. These methods may, however, model in some way the fabrics of sand fills densified in layers.

IX. DISCUSSION

The results presented in the preceding sections have shown the following relationships for Monterey No. 0 sand.

1. The fabrics produced by each of the sample preparation methods studied were quite reproducible.
2. Samples prepared to both 50 percent and 80 percent relative density by dry pluviation are considerably weaker under undrained cyclic loading than samples prepared by moist vibration or by moist tamping.
3. Samples prepared by dry pluviation are less stiff, compress more prior to dilation (at 50 percent relative density), and dilate less than samples prepared by moist vibration or moist tamping when tested in drained triaxial compression.
4. Differences in the drained stress-strain and volume change-strain behavior are considerably less at 80 percent relative density for different methods of compaction than are differences in the liquefaction behavior.
5. Preferred orientations of particle long axes develop in the horizontal direction for each of the methods of compaction studied.
6. The intensity of preferred long axis orientation, as measured by vector length L in Table 4, increases in the order moist vibration, moist tamping, dry pluviation, with the particles very nearly randomly oriented in the samples prepared by moist vibration.
7. At a given relative density the more random the particle orientation (lower L) the higher the strength under undrained

cyclic triaxial loading and the greater the stiffness and dilation in drained triaxial compression.

8. At a relative density of 50 percent the proportion of interparticle contact plane orientations in the range 0 to ±30° of the horizontal increases in the order pluviation, moist tamping, and moist vibration. The proportion of contact planes oriented in these directions is greater than at other orientations for all methods of compaction.
9. At 80 percent relative density a greater proportion of interparticle contacts is oriented at 0 to ±30° with the horizontal for dry pluviation than for moist tamping, even though the strength in cyclic loading is considerably greater for samples prepared by moist tamping.
10. Substantial variations in sample density in a longitudinal direction could be seen in X-radiographs, and these variations differed for sample preparation by the different methods.

These results taken collectively indicate that the fabric elements represented by particle long axis orientation and interparticle contact plane orientation are strongly related to both the undrained strength under cyclic loading and the stiffness and volume change behavior in drained triaxial compression. Although in all cases studied in this investigation higher strengths under the triaxial stress states used were associated with a greater randomness in particle long axis orientations, the relations between strength and interparticle contact orientations were reversed for samples at 50 percent and 80 percent relative density. It should be noted that these findings are somewhat at variance with those for the less extensive and preliminary fabric-strength study reported by Mulilis et al (1975).

There are other aspects of sample preparation methods and the fabric differences studied here that could contribute to the observed differences in strength and volume change behavior. Several observations were made during the study of thin sections that may be potentially significant. Insufficient study of them has been made to allow detailed quantitative analysis. They are

1. Of the order of 0.5 to 1.0 percent of the grains in samples prepared by moist tamping and moist vibration appeared cracked or fractured. A schematic drawing of the nature of this observation is shown in Fig. 34. A detailed macroscopic study of grains before and after compaction would be required to confirm that cracking resulted from compaction stresses.
2. Larger voids were observed in the horizontal thin sections than in vertical sections. Figure 35 is a schematic diagram of an isolated large pore.
3. Grain and contact orientations are less easily determined in dense than in loose regions.

There are other fabric-related factors and observations that have not yet been studied in detail, but which may have a major influence on the liquefaction behavior of sand. They are:

1. Variable void ratios within samples. The influences of both large and small inhomogeneities within samples in relation to a given average relative density remain largely unknown.
2. Segregation of different particle sizes within the sample.
3. Influences of stress history, including overconsolidation, and types of stress system. Triaxial loading was used for this investigation. Fabric-liquefaction relationships for deformation in simple shear may not be the same.

4. Different particle cluster arrangements as a result of different preparation methods. Pore size distribution measurements might provide information relative to this, as well as relative to factors 1 and 2 above.

5. These studies as well as those by Mulilis et al (1975) and Ladd (1975)* show that wet preparation methods consistently give higher strengths than do dry preparation methods. Both moist tamping and moist vibration give higher strength than do dry tamping or dry vibration to the same density. Ladd's studies show that the rate of strain development with increased numbers of loading cycles was the same for samples of a uniform sand prepared by all methods to a relative density of 60 percent. On the other hand the rate of strain development was quite different for dry fabricated and moist fabricated samples of a more well graded sand prepared to a relative density of 80 percent.

6. Chemical effects at interparticle contacts that may develop in moist samples owing to abrasion during tamping or vibration and subsequent consolidation may be of major importance. Chemical analysis and high resolution electron microscopy of particle surfaces before and after compaction might provide useful data on chemical and surface texture phenomena.

7. The influence of sand type to include particle shape and gradation. The Monterey No. 0 sand used for this study is uniform and composed of rounded grains which are nearly equidimensional.

Finally, it is clear that careful study is needed of the fabrics of naturally occurring sand deposits and sand fills in the field if

---

*Ladd, R. S. (1975), personal communication.

proper characterization of their behavior by tests on reconstituted samples in the laboratory is to be achieved. In-situ injection of sands in the field to stabilize the fabric prior to sampling should enable recovery of samples suitable for detailed study.

X. CONCLUSION

This study has established that the undrained strength of Monterey No. 0 sand under cyclic triaxial loading and the drained triaxial stress-strain and volume change, strain behavior bear specific relationships to the sand fabric, which in turn is determined by the method of sample preparation. Of three sample preparation methods investigated moist vibration gave the most random orientations of particle long axes. Dry pluviation resulted in distinct preferred orientation of particle long axes in the horizontal direction. Moist tamping gave intermediate values. The highest strengths were associated with the most random particle orientations.

The distribution of interparticle contact plane orientations appears to be an important factor influencing the resistance of a sand to liquefaction. However, the influence of contact orientation distributions appears to vary depending on relative density.

A clear relationship exists between the stiffness and volume change characteristics in drained triaxial compression and the resistance to liquefaction under undrained triaxial cyclic loading. This correlation is stronger at a relative density of 50 percent than at a relative density of 80 percent.

Additional factors such as pore size and particle cluster size distribution, particle breakage during compaction, particle size segregation within samples, and chemical effects at interparticle contacts need further study in relation to their influences on strength and liquefaction behavior.

Direct application of the results of this study to the selection of the appropriate method for preparation of reconstituted samples must await the analysis of the fabrics of undisturbed samples from the field.

REFERENCES

Arthur, J. F. and Menzies, B. K. (1972) "Inherent Anisotropy in a Sand," Geotechnique, Vol. 22, No. 1, pp. 115-128.

Curry, J. R. (1956) "The Analysis of Two-dimensional Orientation Data," Journal of Geology, Vol. 64, pp. 117-131.

Kellerhals, R. and Bray, D. (1971) "Sampling Procedures for Coarse Fluvial Sediments," Journal of the Hydraulics Division, ASCE, August, pp. 1165-1180.

Koch, G. S. and Link, R. F. (1970) Statical Analysis of Geological Data, John Wiley & Sons, Inc., New York, Vol. 1, 375 p., Vol. 2, 438 p.

Ladd, R. S. (1974) "Specimen Preparation and Liquefaction of Sand," Journal of the Geotechnical Engineering Division, ASCE, Vol. 100, No. GT10, pp. 1180-1184.

Mahmood, A. (1973) "Fabric-Mechanical Property Relationships in Fine Granular Soils," Ph.D. Dissertation, University of California, Berkeley.

Mahmood, A. and Mitchell, J. K. (1974) "Fabric-Property Relationships in Fine Granular Materials," Clays and Clay Minerals, Vol. 22, No. 516, pp. 397-408.

Miller, R. L. and Kahn, J. S. (1962) Statistical Analysis in the Geological Sciences, John Wiley & Sons, Inc., New York, 483 p.

Mulilis, J. P., Chan, C. K. and Seed, H. B. (1975) "The Effects of Method of Sample Preparation on the Cyclic Stress-Strain Behavior of Sands," Report No. EERC 75-18, University of California, Berkeley, July, 1975.

Oda, M. (1972a) "Initial Fabrics and Their Relations to Mechanical Properties of Granular Materials," Soils and Foundations, Vol. 12, No. 1, pp. 17-37.

Oda, M. (1972b) "The Mechanism of Fabric Changes During Compressional Deformation of Sand," Soils and Foundations, Vol. 12, No. 2, pp. 1-18.

Pincus, H. J. (1953) "The Analysis of Aggregates of Orientation Data in the Earth Sciences," Journal Geol., Vol. 61, No. 6, November, pp. 482-509.

Turner, F. J. and Weiss, L. E. (1963) Structural Analysis of Metamorphic Tectonites, McGraw-Hill Book Co., New York, pp. 194-255.

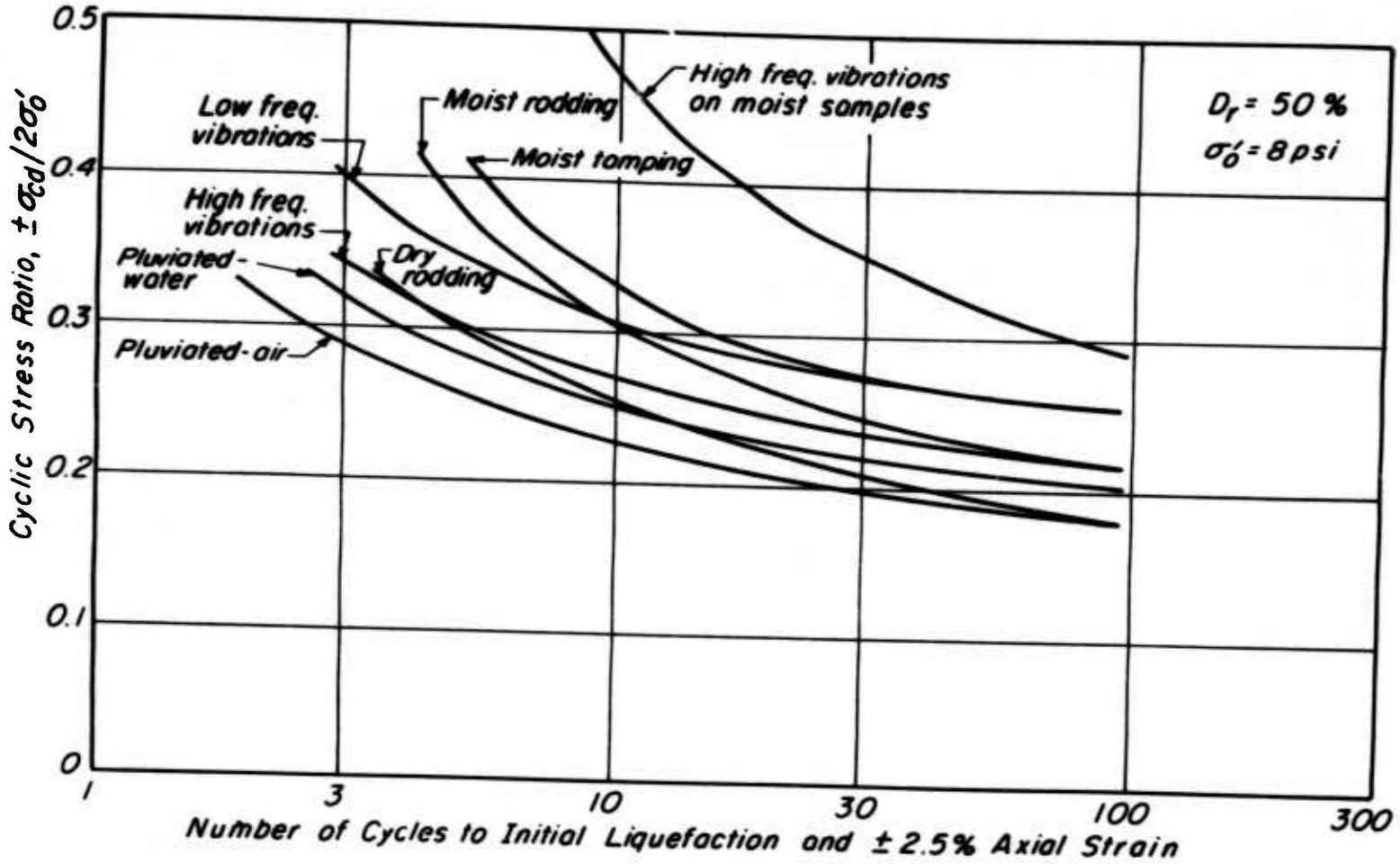

FIG. 1 COMPARISON OF STRENGTHS UNDER CYCLIC LOADING FOR SAMPLES PREPARED BY DIFFERENT METHODS. MONTEREY NO. 0 SAND AT A RELATIVE DENSITY OF 50%

(Mulilis et al, 1975)

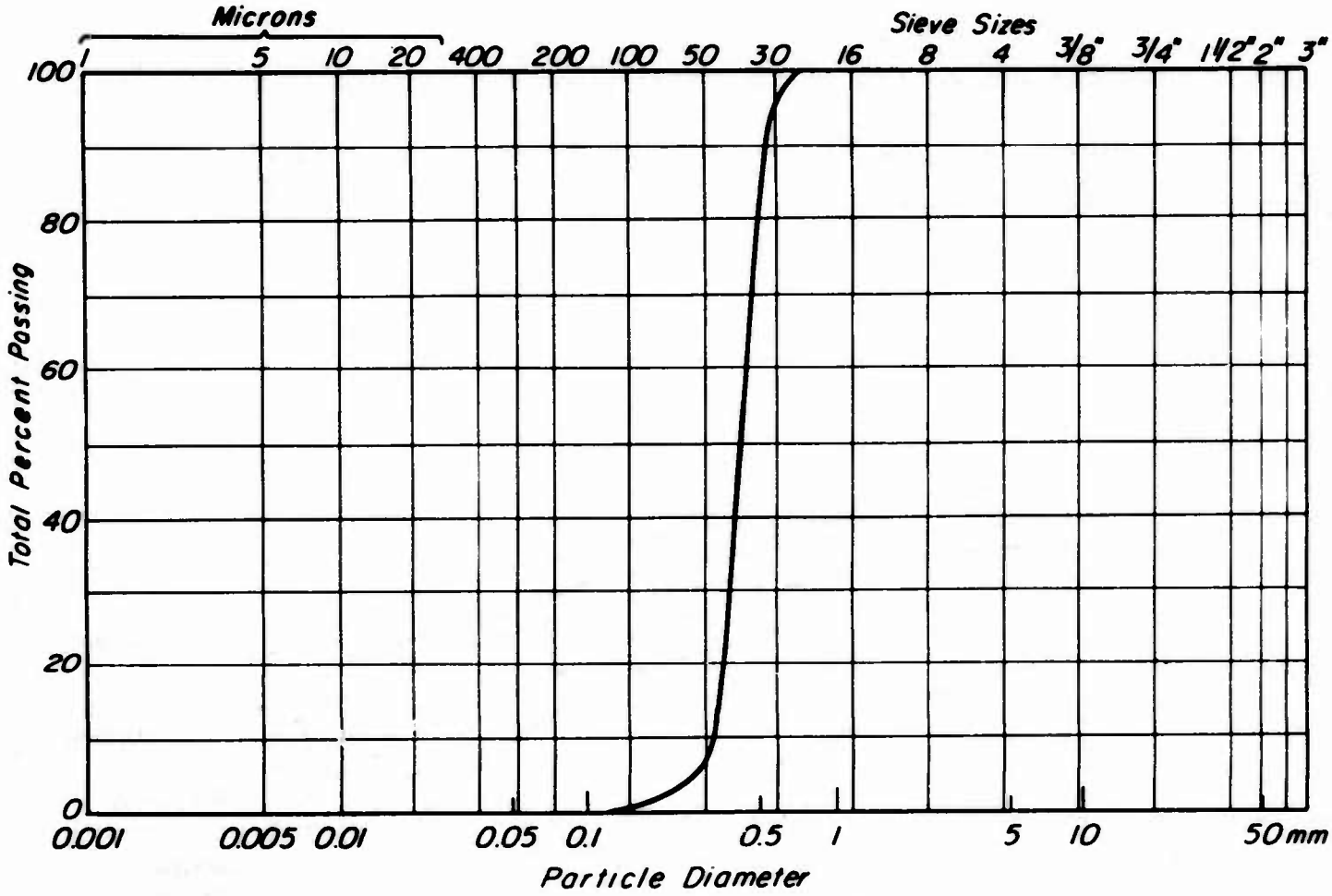

FIG. 2 GRAIN SIZE DISTRIBUTION OF MONTEREY NO. 0 SAND

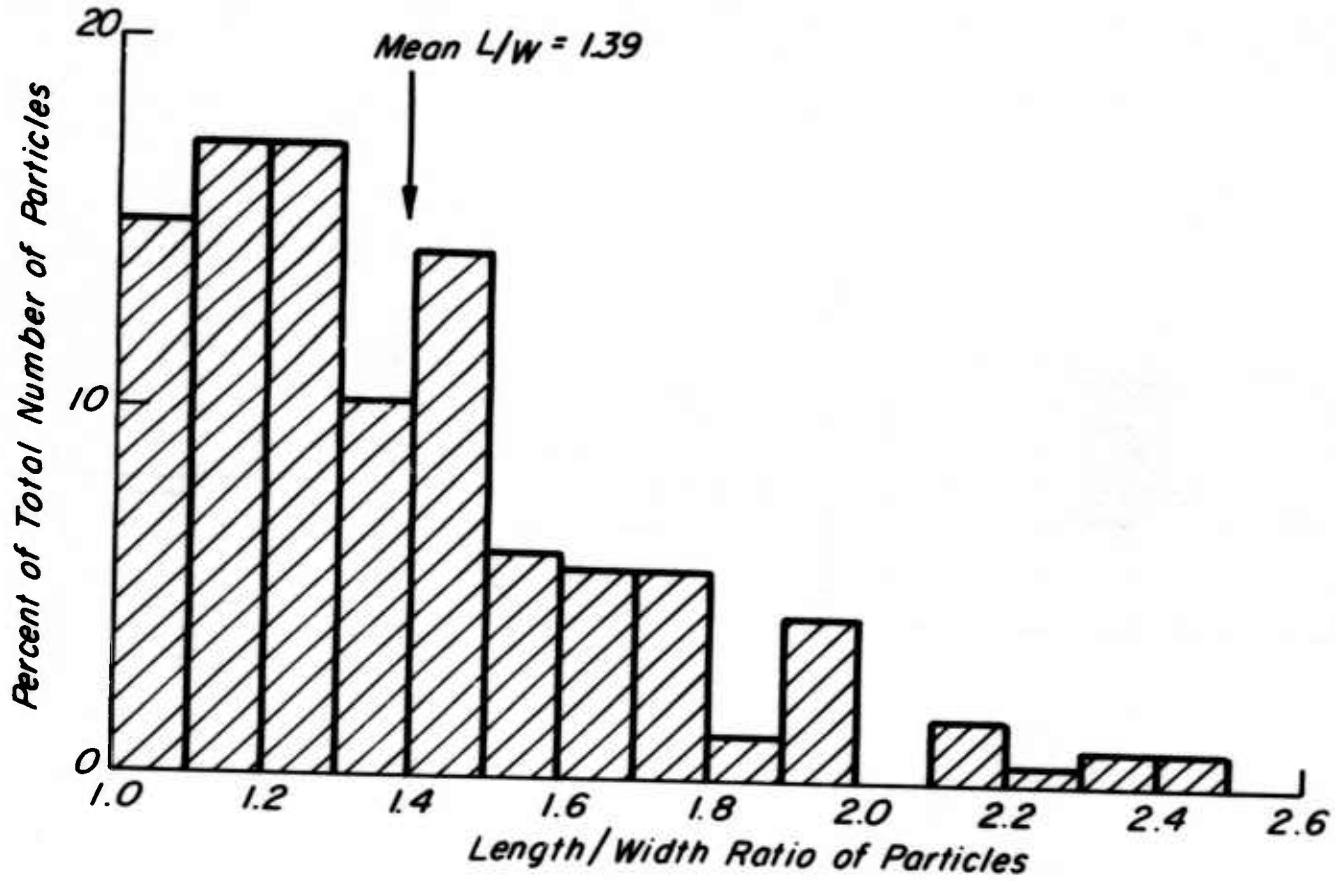

FIG. 3 GRAIN SHAPE DISTRIBUTION OF MONTEREY NO. 0 SAND (227 PARTICLES) (from Mahmood, 1973)

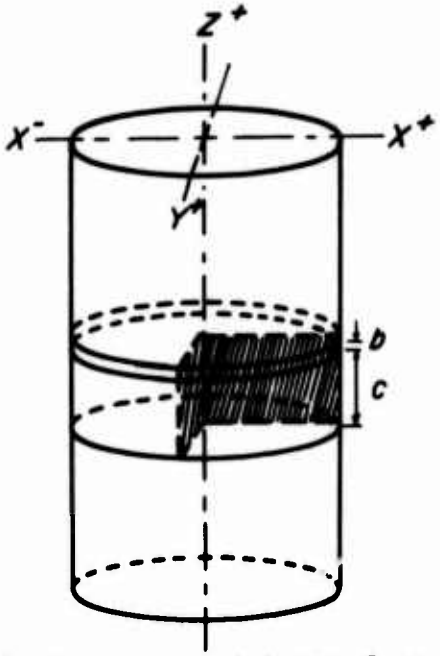

(a) Locations of Initial Cuts

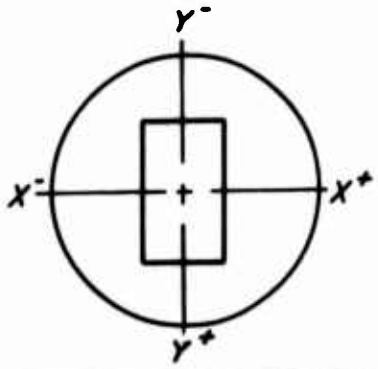

(b) Horizontal Section

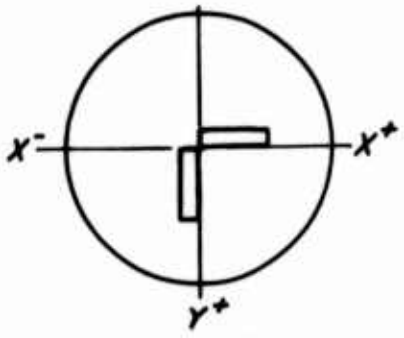

(c) Vertical Sections

FIG. 4 THIN SECTION LOCATIONS FROM WITHIN RESIN-IMPREGNATED SAMPLES

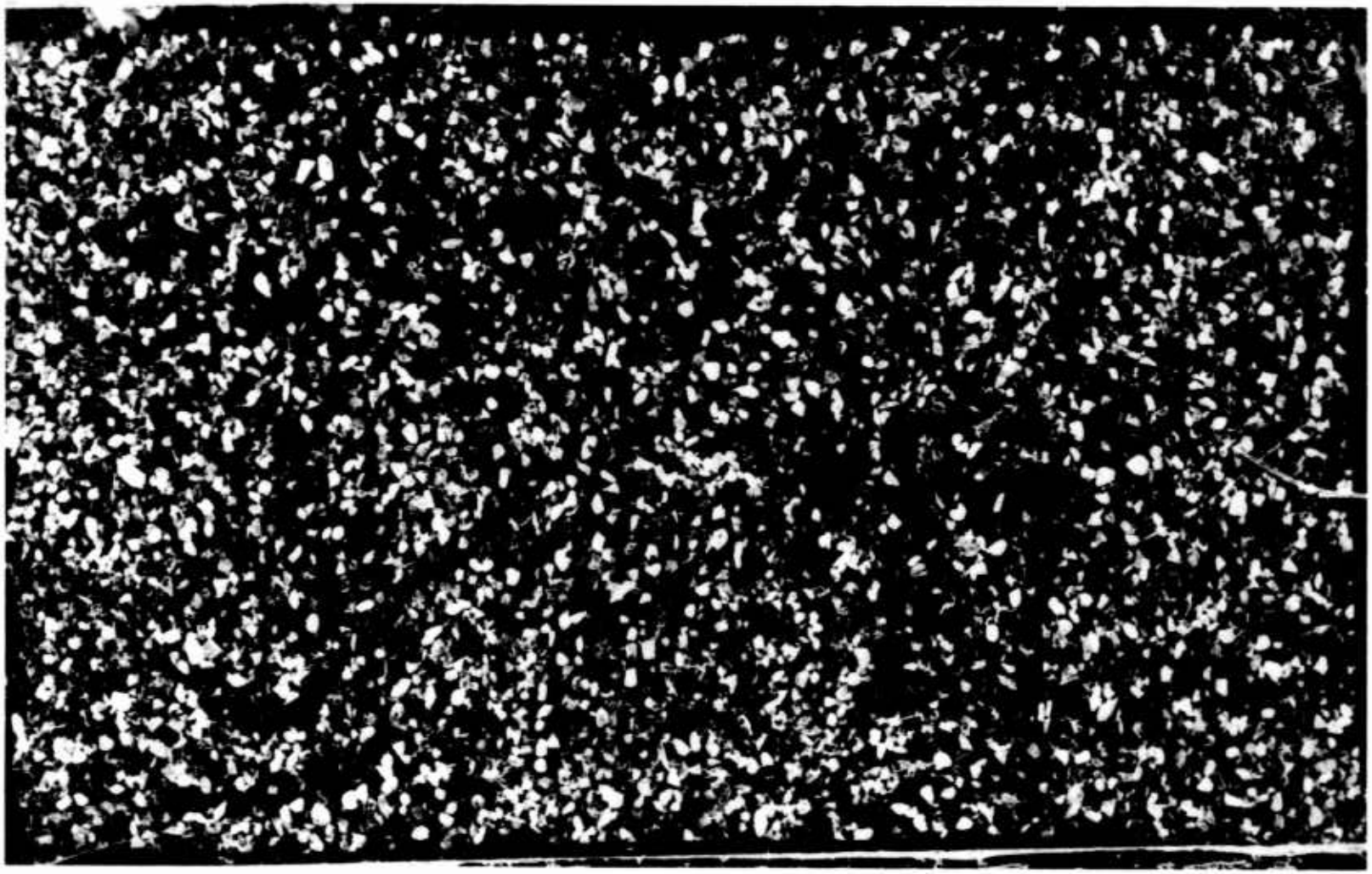

FIG. 5 PHOTOMICROGRAPH OF VERTICAL THIN SECTION FROM SAMPLE PREPARED BY PLUVIATION (50% RELATIVE DENSITY)

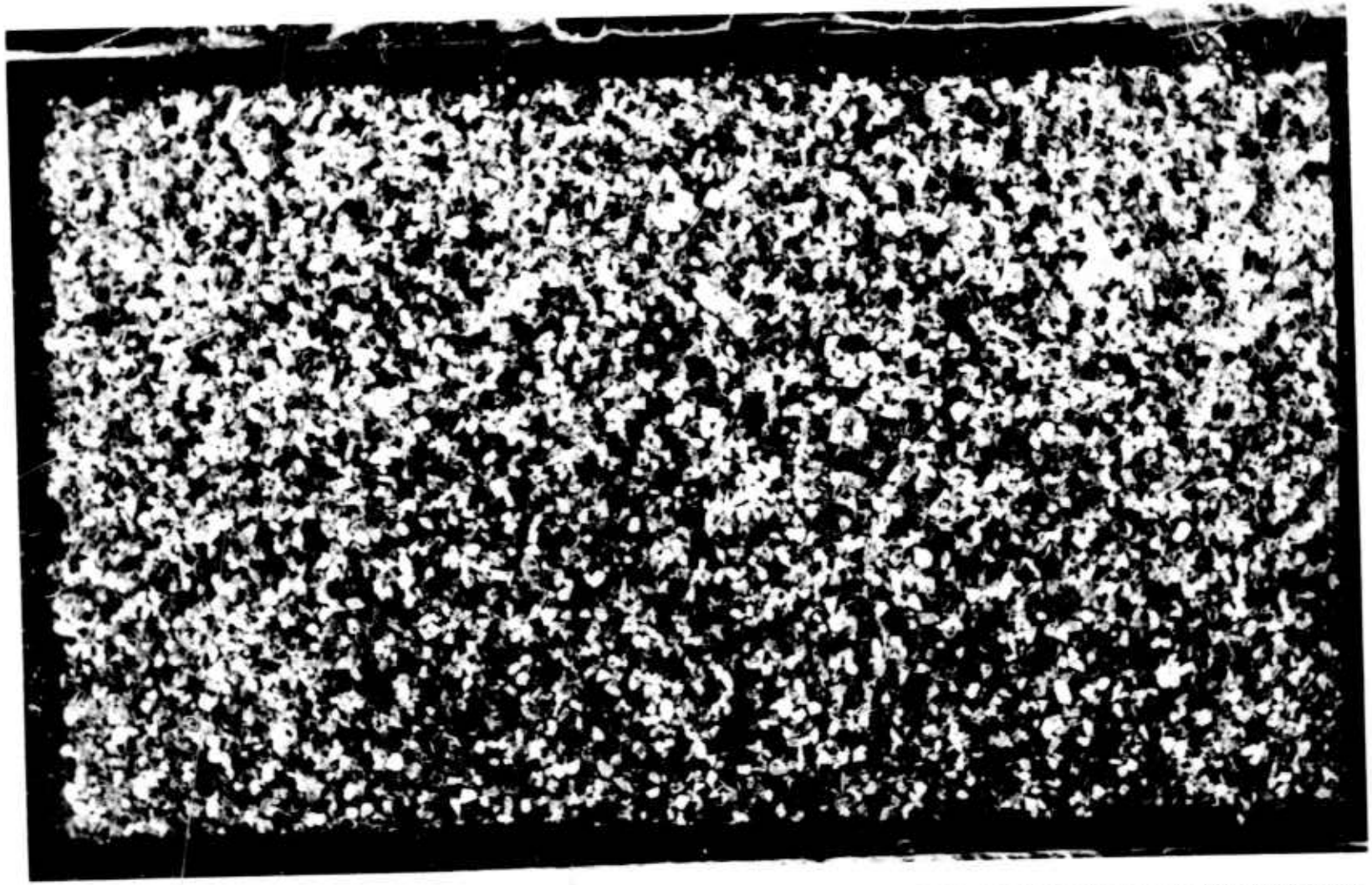

FIG. 6 PHOTOMICROGRAPH OF VERTICAL THIN SECTION FROM SAMPLE PREPARED BY MOIST TAMPING (50% RELATIVE DENSITY)

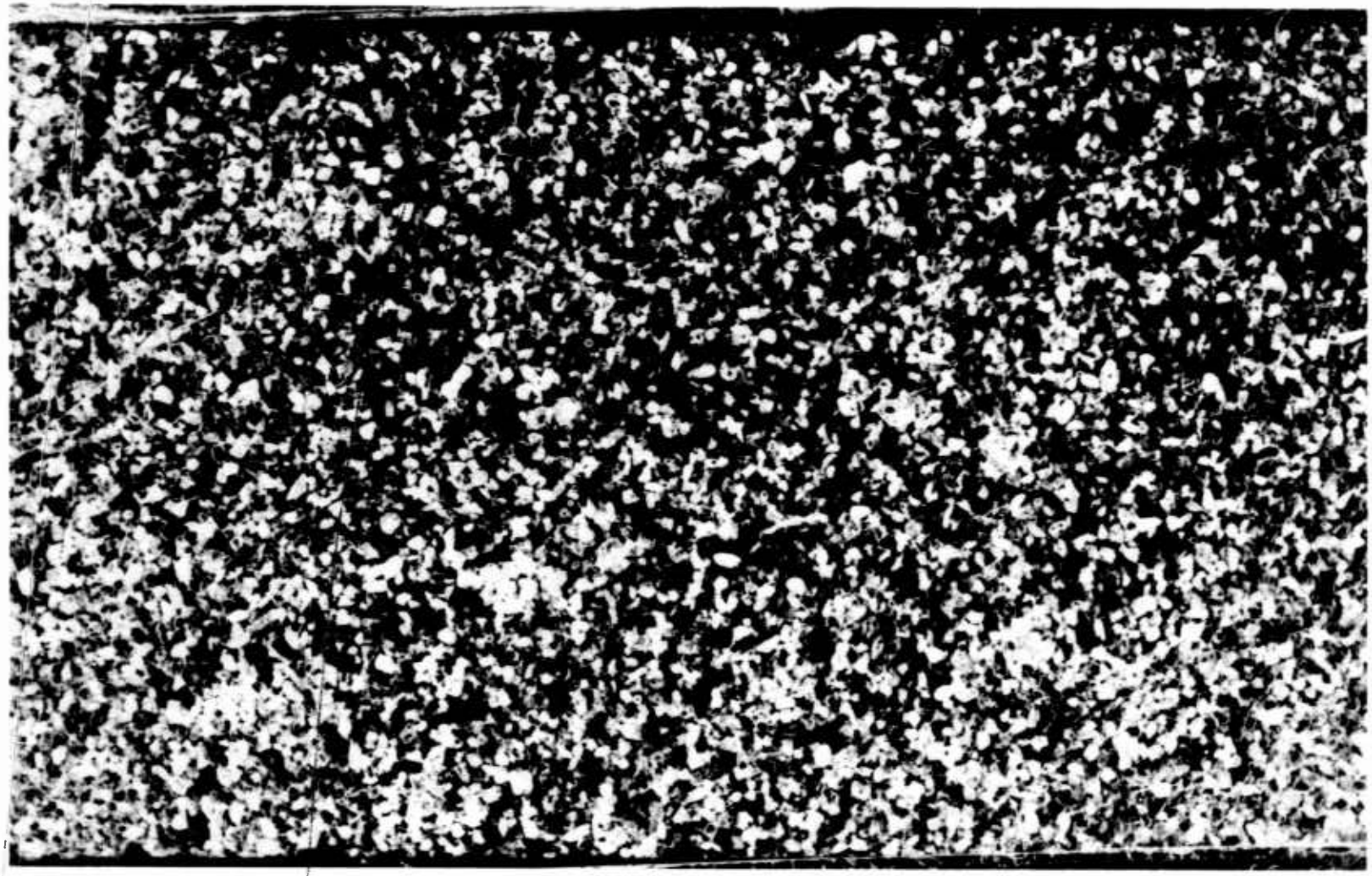

FIG. 7 PHOTOMICROGRAPH OF VERTICAL THIN SECTION FROM SAMPLE PREPARED BY MOIST VIBRATION (50% RELATIVE DENSITY)

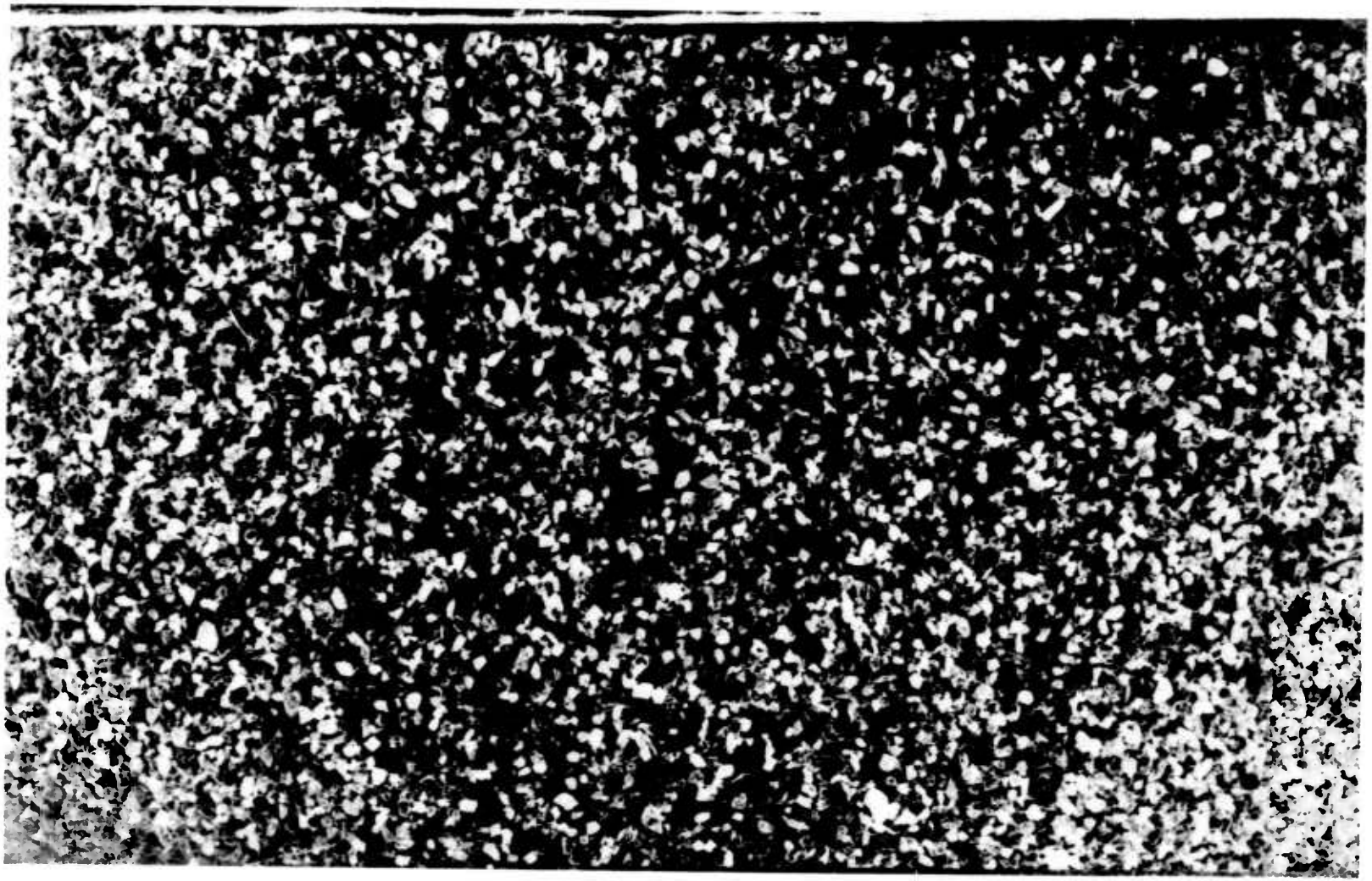

FIG. 8 PHOTOMICROGRAPH OF VERTICAL THIN SECTION FROM SAMPLE PREPARED BY PLUVIATION (80% RELATIVE DENSITY)

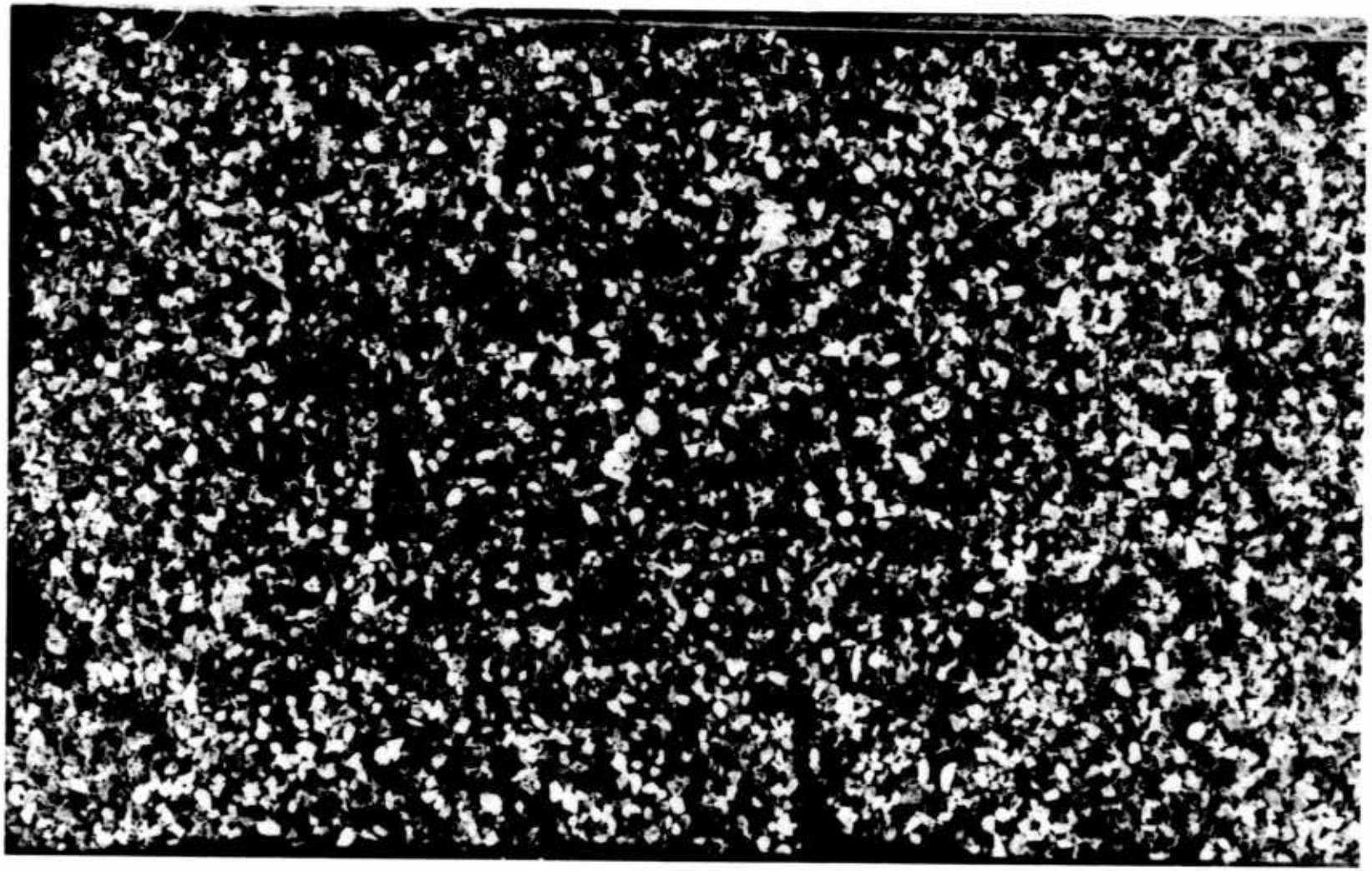

FIG. 9 PHOTOMICROGRAPH OF VERTICAL THIN SECTION FROM SAMPLE PREPARED BY MOIST TAMPING (80% RELATIVE DENSITY)

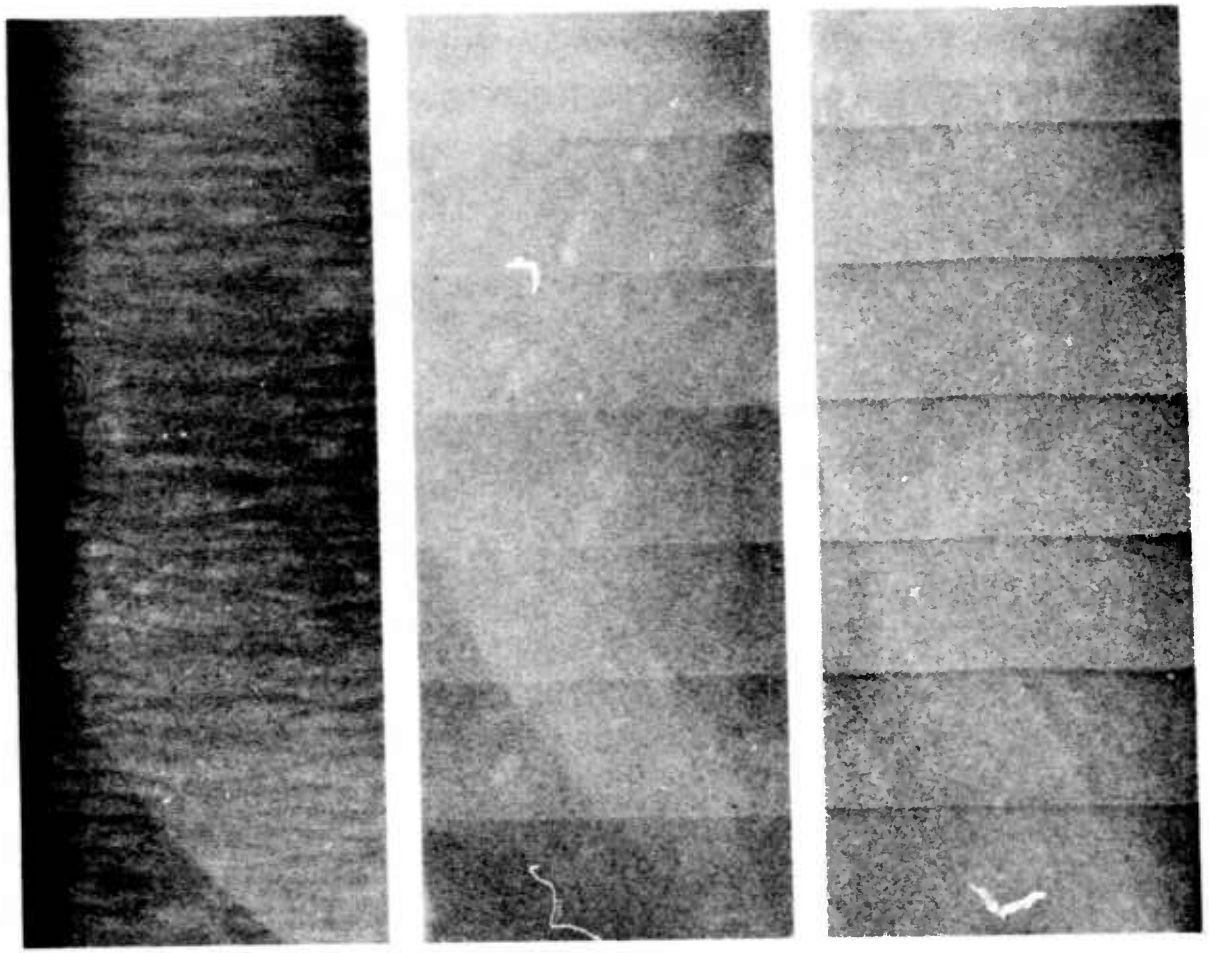

Pluviated Moist Tamped Moist Vibrated

FIG. 10 X-RADIOGRAPHS OF LONGITUDINAL SECTIONS FROM SAMPLES AT 50% RELATIVE DENSITY

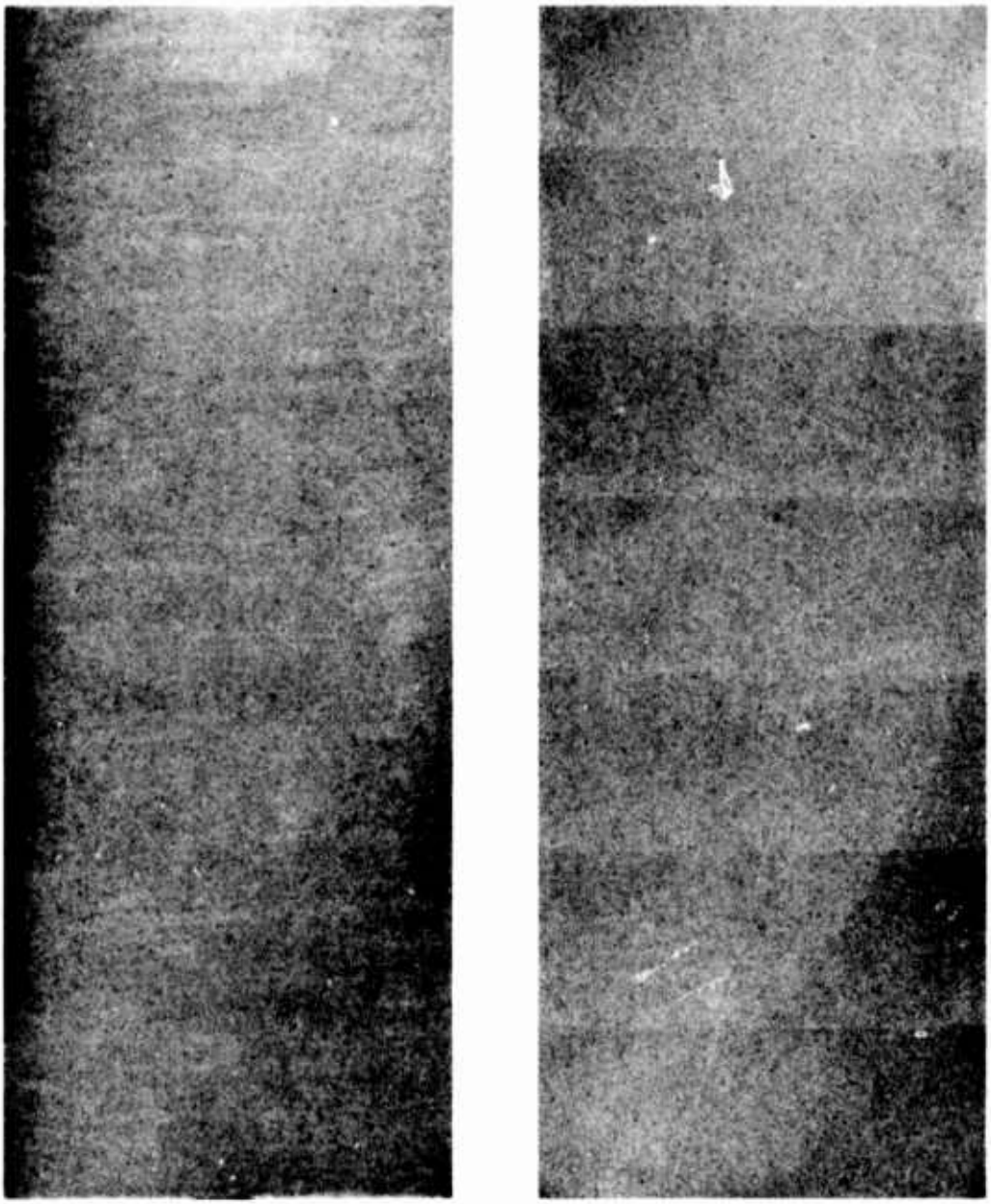

Pluviated D_r = 80%

Moist Tamped D_r = 80%

FIG. 11 X-RADIOGRAPHS OF LONGITUDINAL SECTIONS FROM SAMPLES AT 80% RELATIVE DENSITY

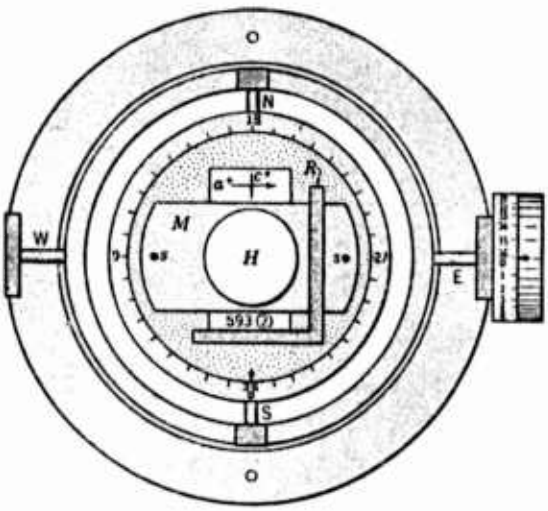

FIG. 12 UNIVERSAL STAGE LOOKING DOWN THE VERTICAL ROTATION AXIS

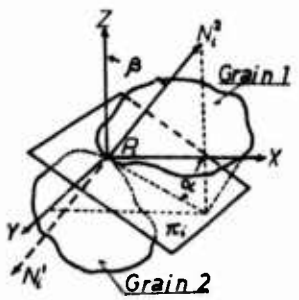

FIG. 13 MEASUREMENT OF NORMALS (N_i^1, N_i^2) TO TANGENT PLANE (π_i)

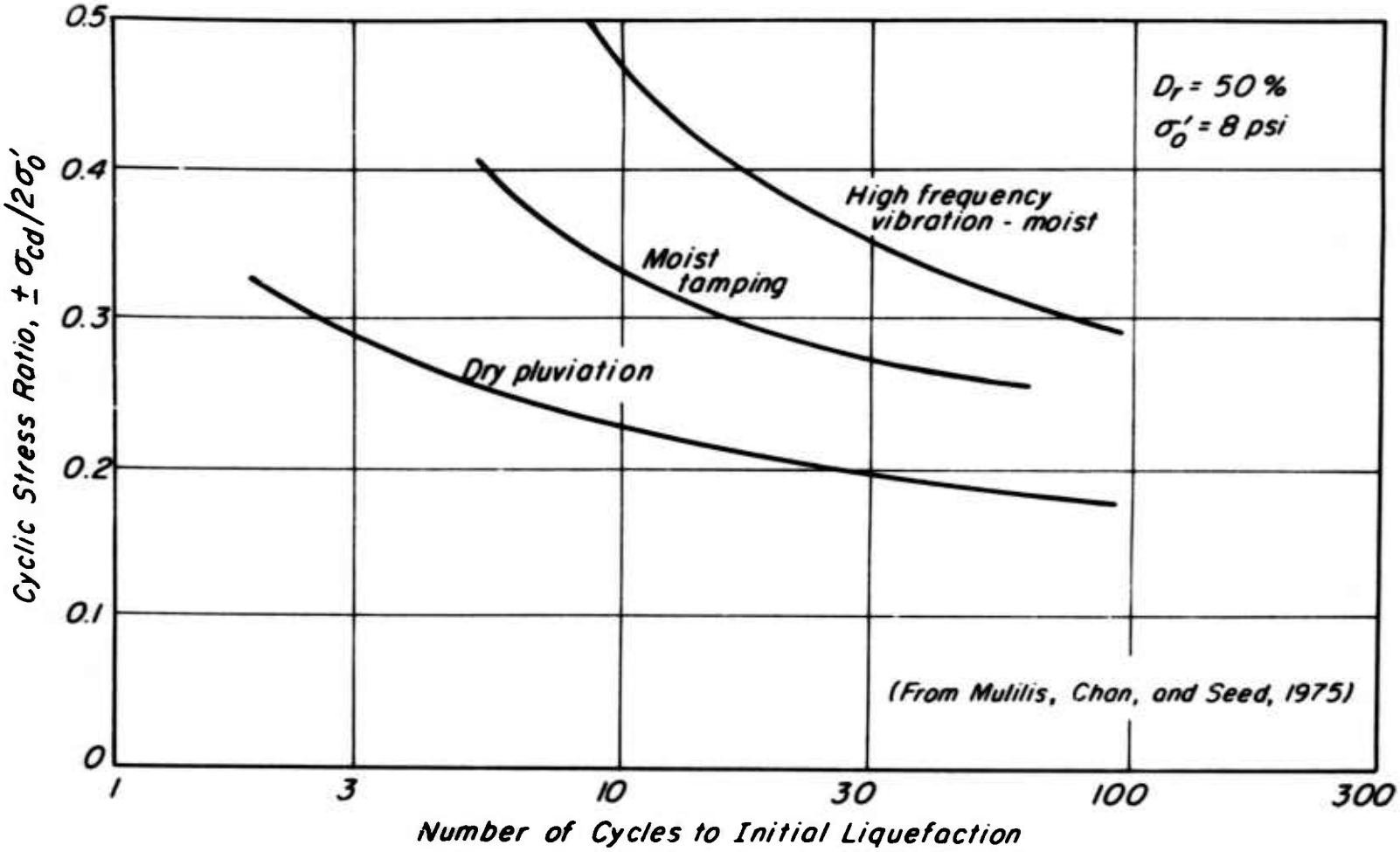

FIG. 14 LIQUEFACTION BEHAVIOR OF MONTEREY NO. 0 SAND PREPARED TO A RELATIVE DENSITY OF 50 BY THREE METHODS

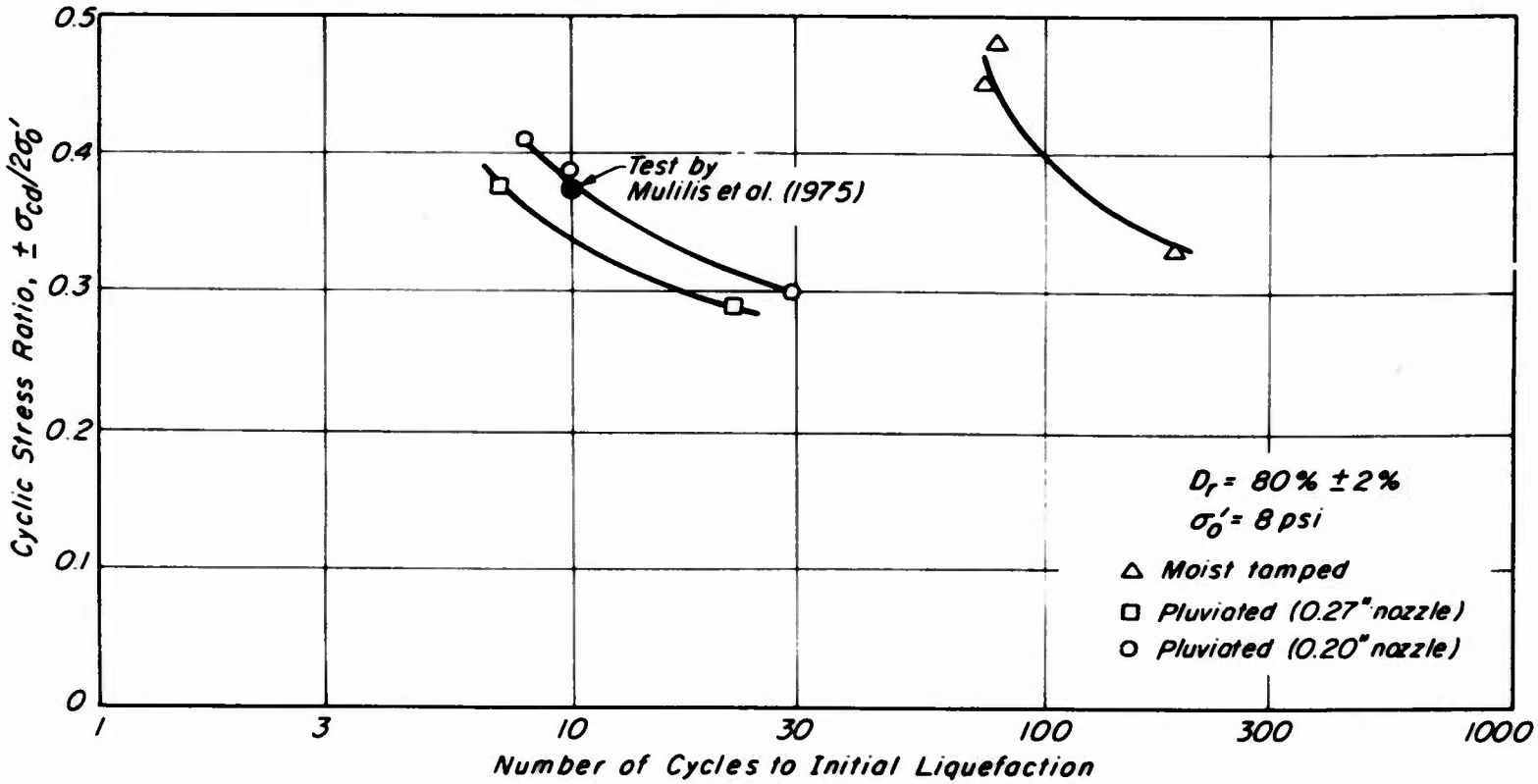

FIG. 15 LIQUEFACTION BEHAVIOR OF MONTEREY NO. 0 SAND PREPARED TO A RELATIVE DENSITY OF 80% BY PLUVIATION AND MOIST TAMPING

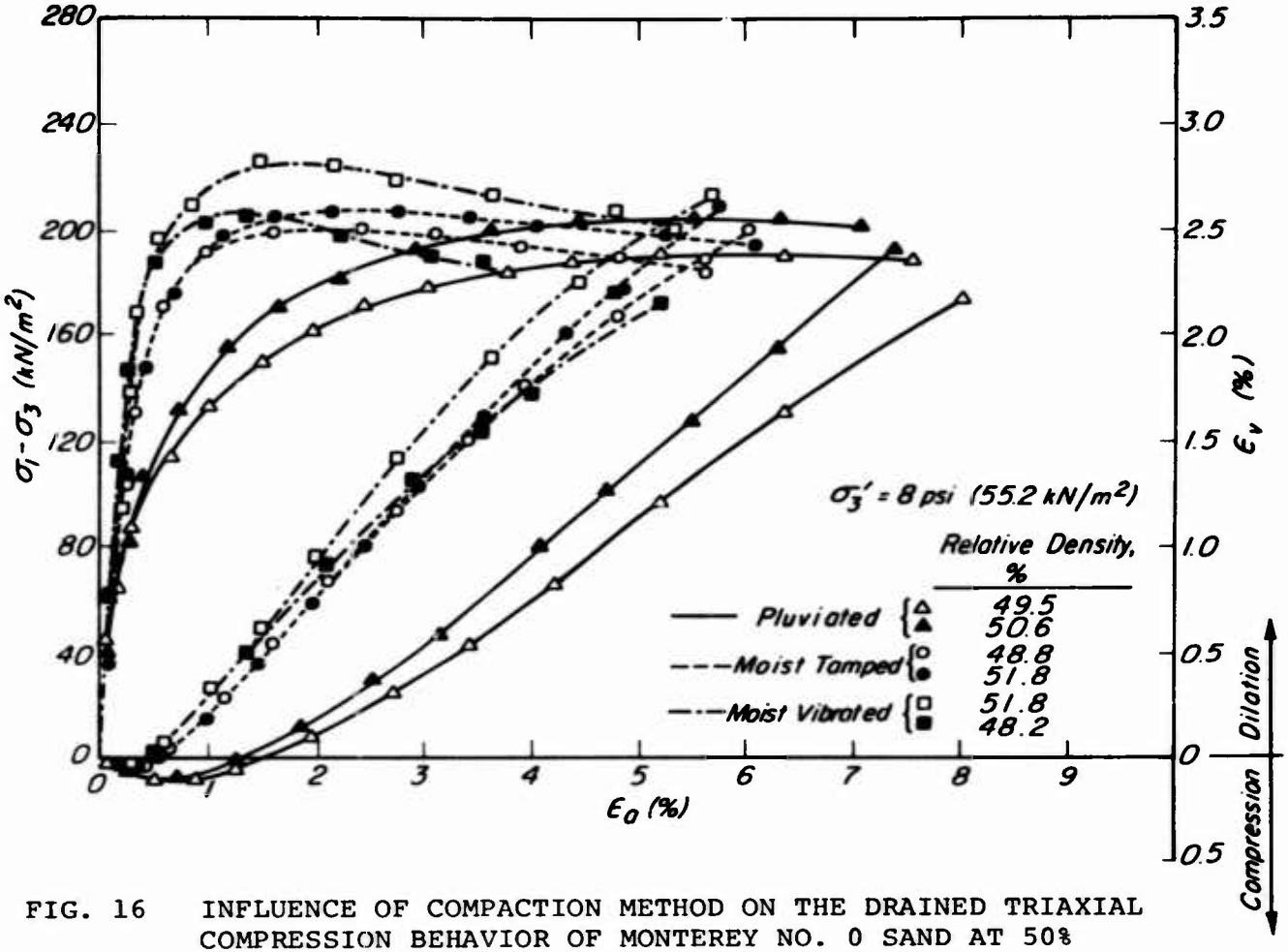

FIG. 16 INFLUENCE OF COMPACTION METHOD ON THE DRAINED TRIAXIAL COMPRESSION BEHAVIOR OF MONTEREY NO. 0 SAND AT 50% RELATIVE DENSITY

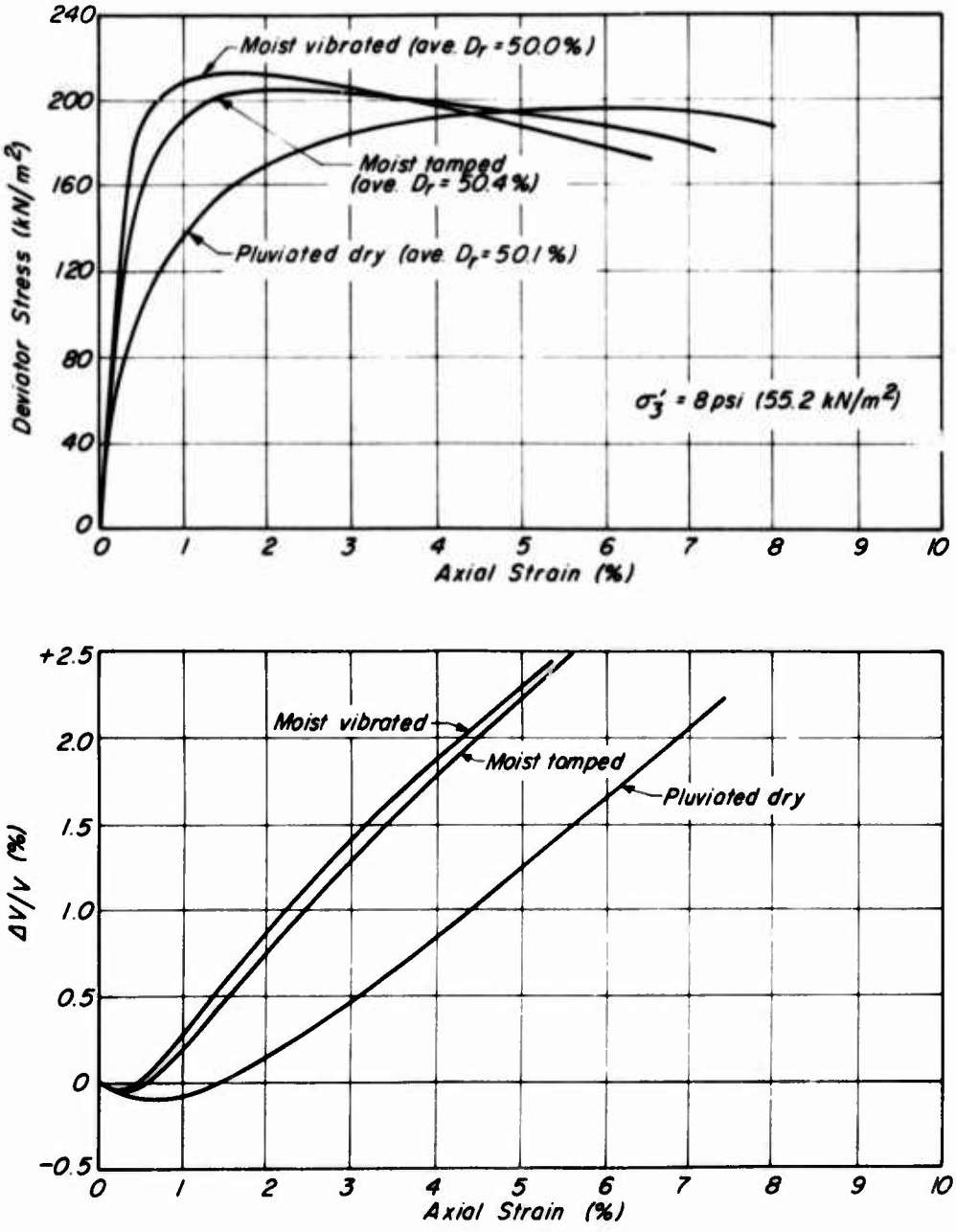

FIG. 17 AVERAGED CURVES BASED ON TWO TESTS ILLUSTRATING THE INFLUENCE OF SAMPLE PREPARATION METHOD ON BEHAVIOR IN DRAINED TRIAXIAL COMPRESSION; MONTEREY NO. 0 SAND AT 50% RELATIVE DENSITY

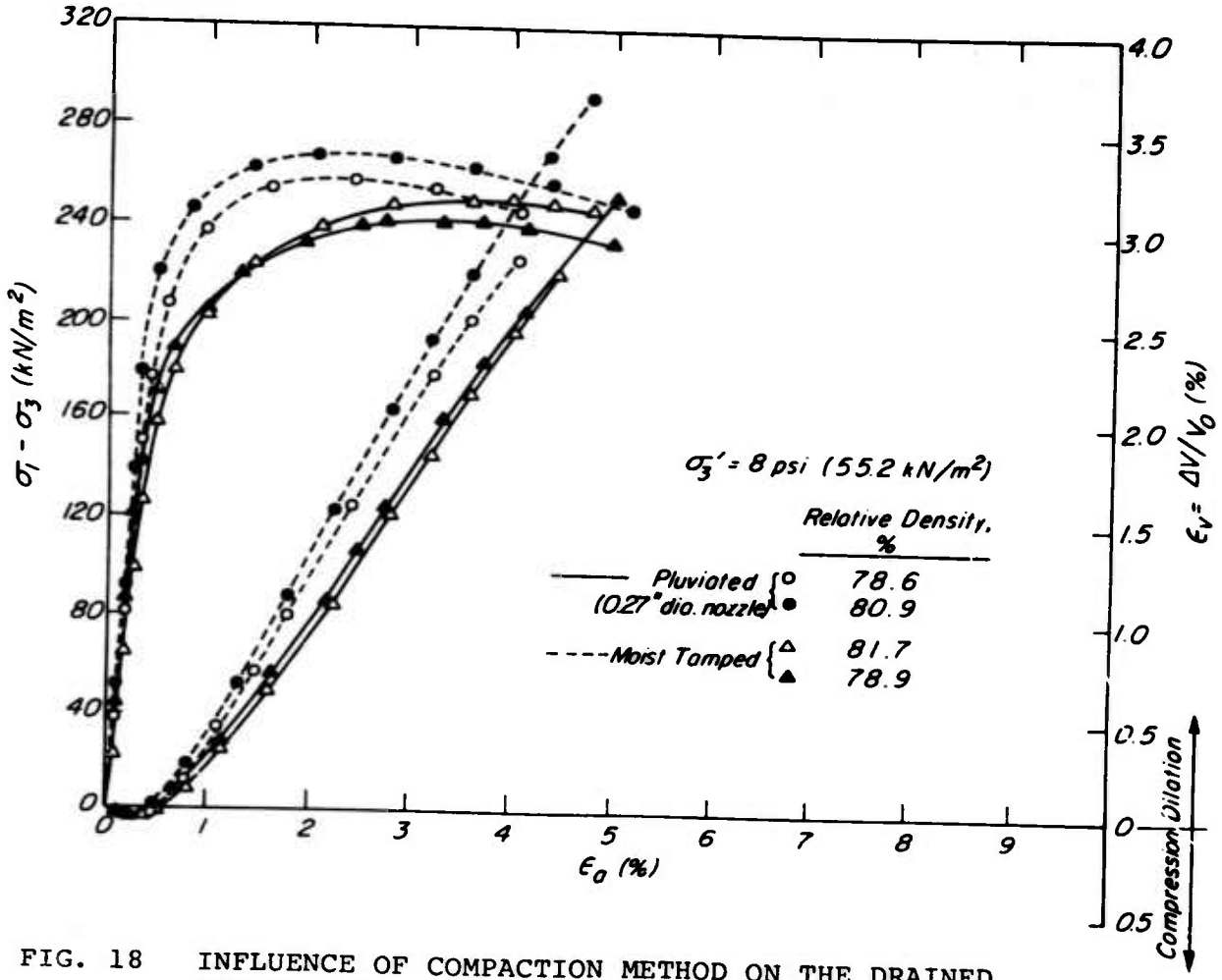

FIG. 18 INFLUENCE OF COMPACTION METHOD ON THE DRAINED TRIAXIAL COMPRESSION BEHAVIOR OF MONTEREY NO. 0 SAND AT 80% RELATIVE DENSITY

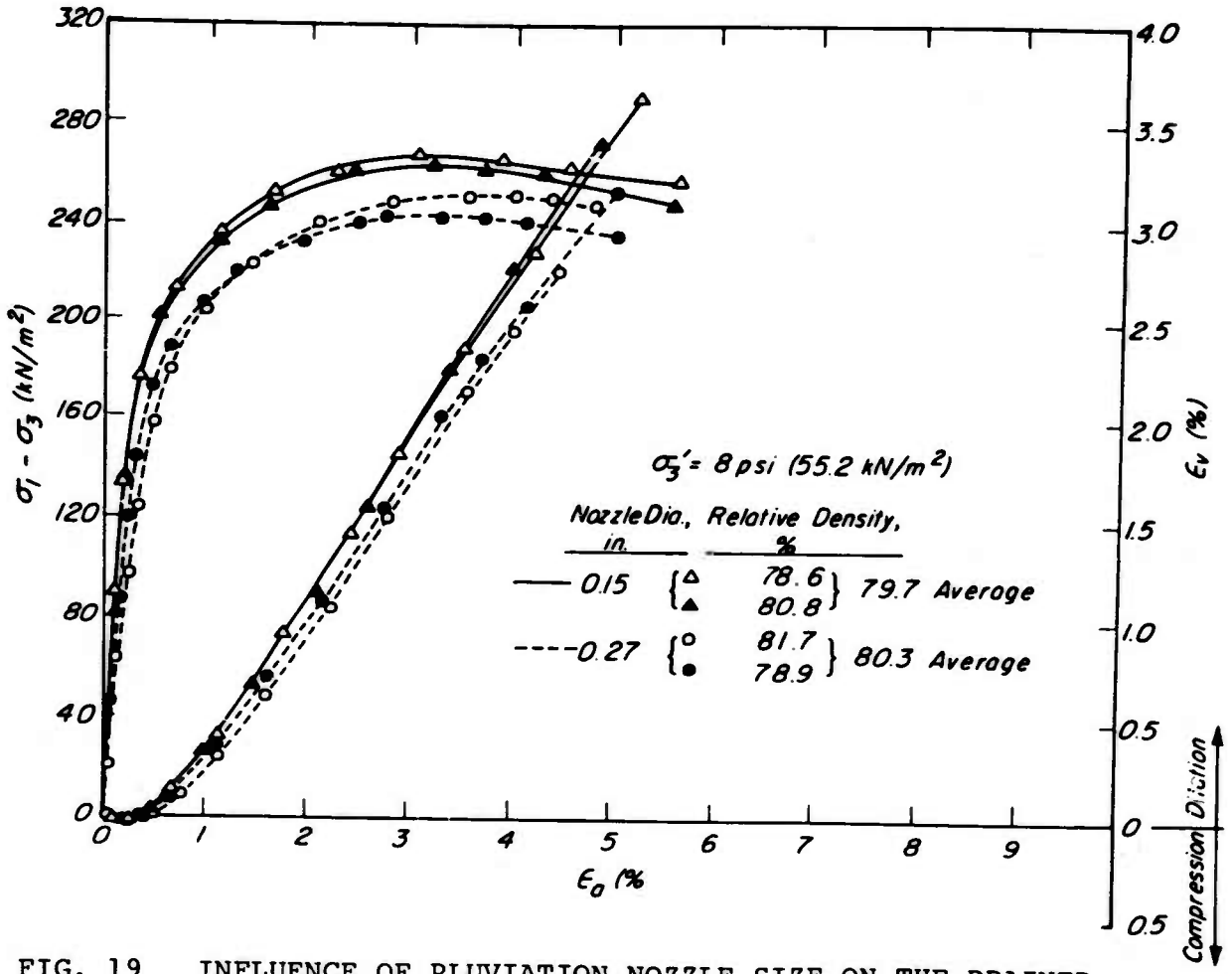

FIG. 19 INFLUENCE OF PLUVIATION NOZZLE SIZE ON THE DRAINED COMPRESSION BEHAVIOR OF MONTEREY NO. 0 SAND AT 80% RELATIVE DENSITY

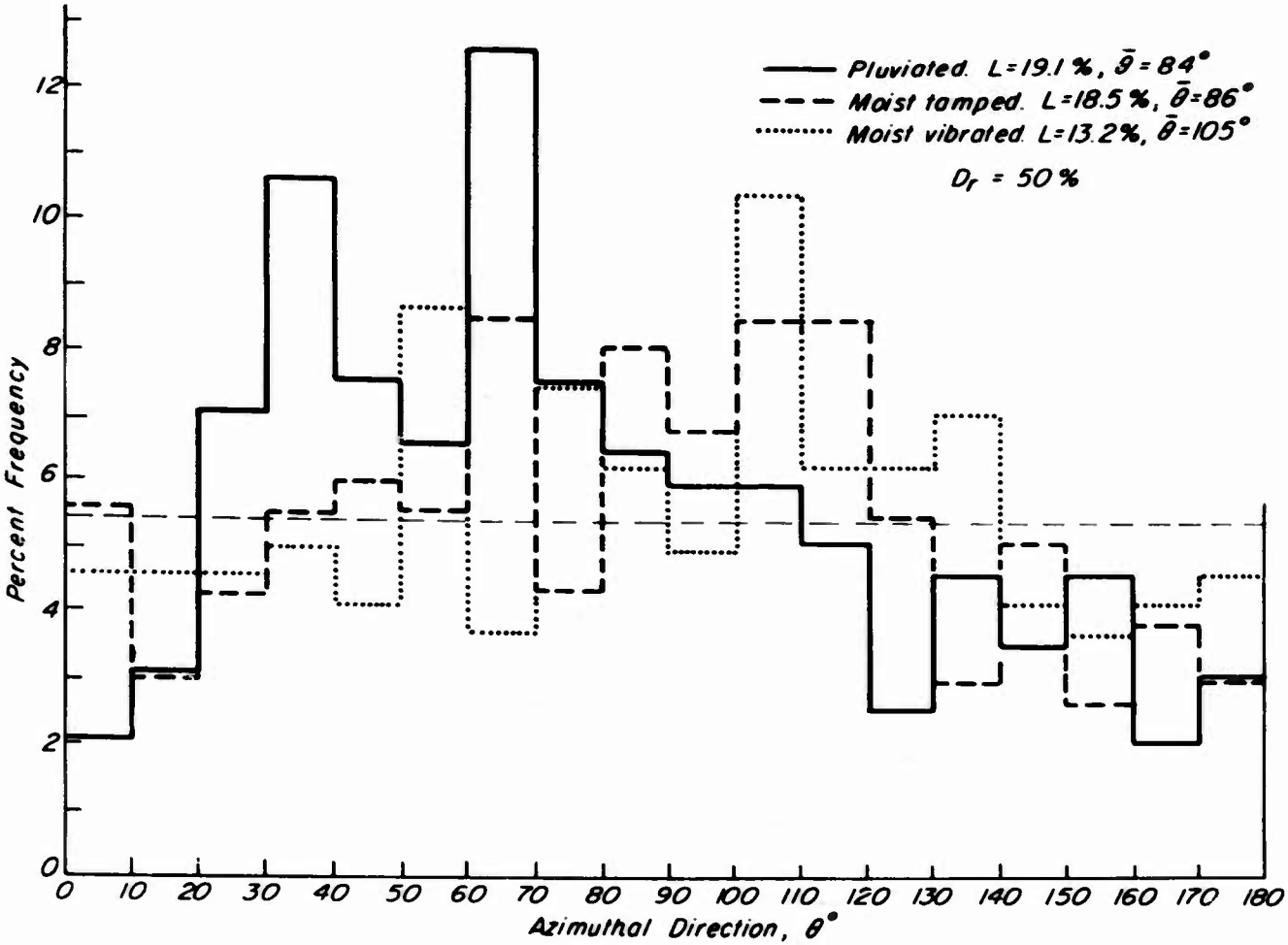

FIG. 20 HISTOGRAMS OF PARTICLE LONG AXIS ORIENTATIONS FOR SAMPLES OF MONTEREY NO. 0 SAND PREPARED TO 50% RELATIVE DENSITY BY DIFFERENT METHODS

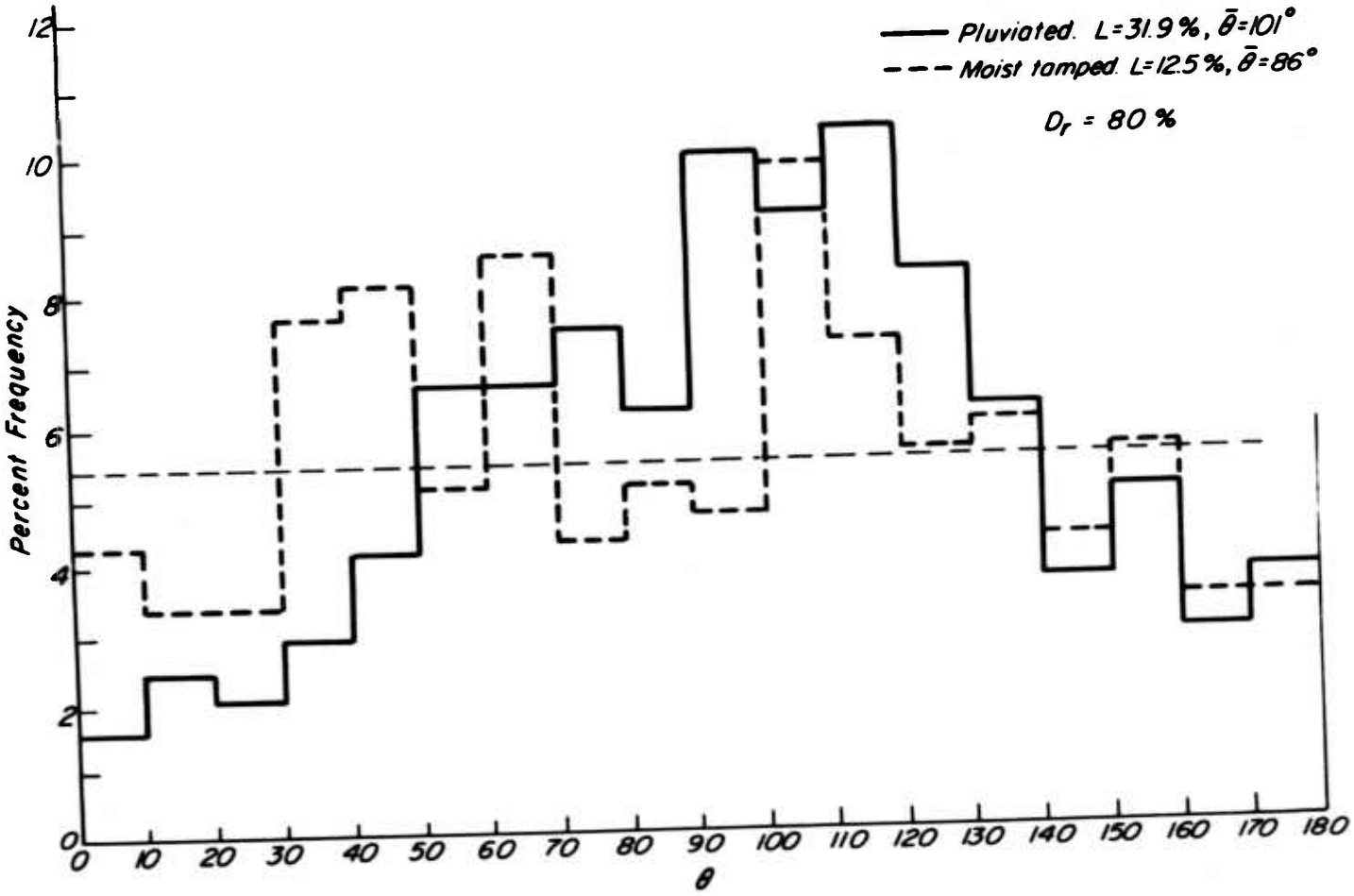

FIG. 21 HISTOGRAMS OF PARTICLE LONG AXIS ORIENTATIONS FOR SAMPLES OF MONTEREY NO. 0 SAND PREPARED TO 80% RELATIVE DENSITY BY DIFFERENT METHODS

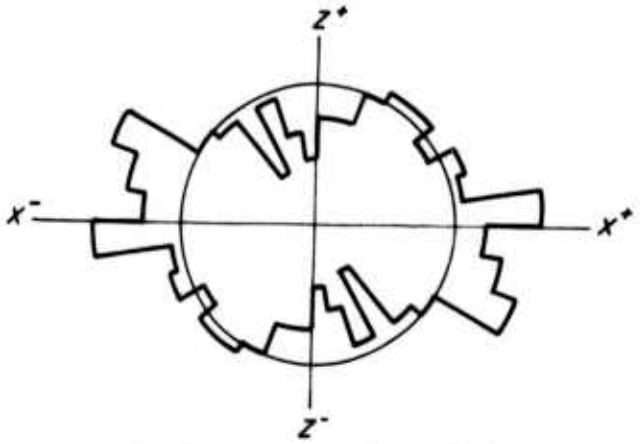

(a) Pluviated. $L = 18.3\%$, $\bar{\theta} = 86°$

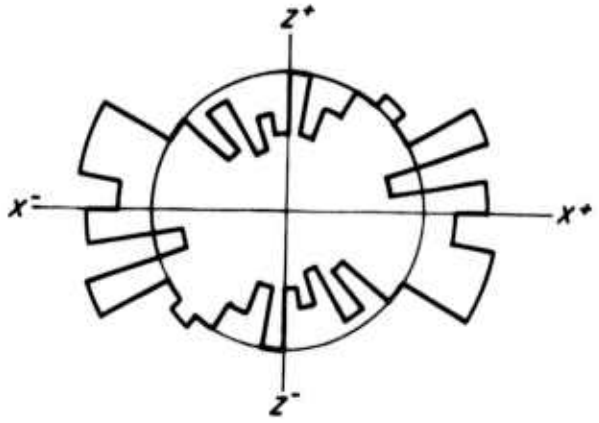

(b) Moist tamped. $L = 18.5\%$, $\bar{\theta} = 86°$

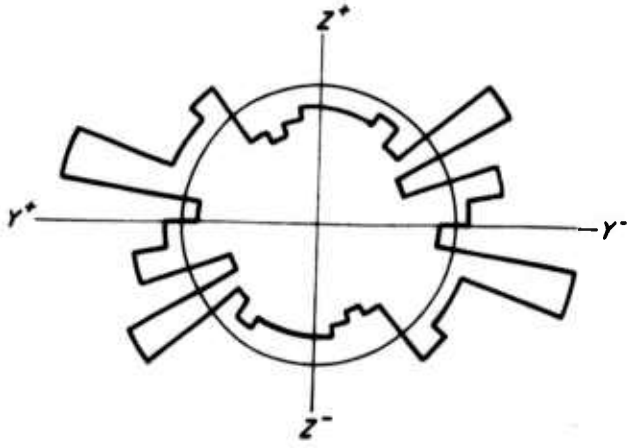

(c) Moist vibrated. $L = 13.2\%$, $\bar{\theta} = 285°$

FIG. 22 ROSE DIAGRAMS OF PARTICLE LONG AXIS ORIENTATIONS FOR SAMPLES OF MONTEREY NO. 0 SAND PREPARED TO 50% RELATIVE DENSITY BY DIFFERENT METHODS

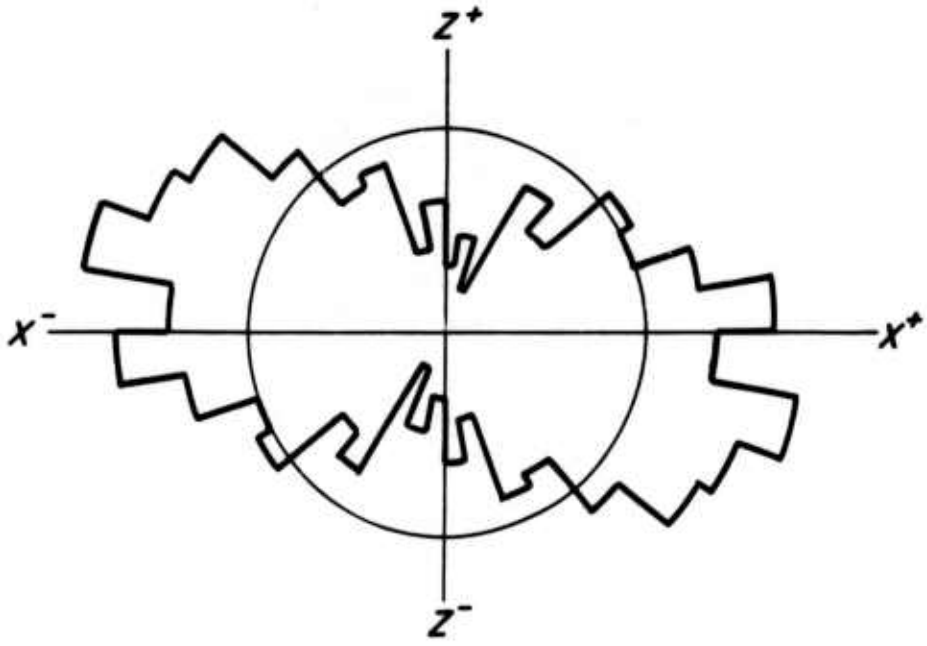

(a) Pluviated. $L=31.2\%$, $\bar{\theta}=281°$

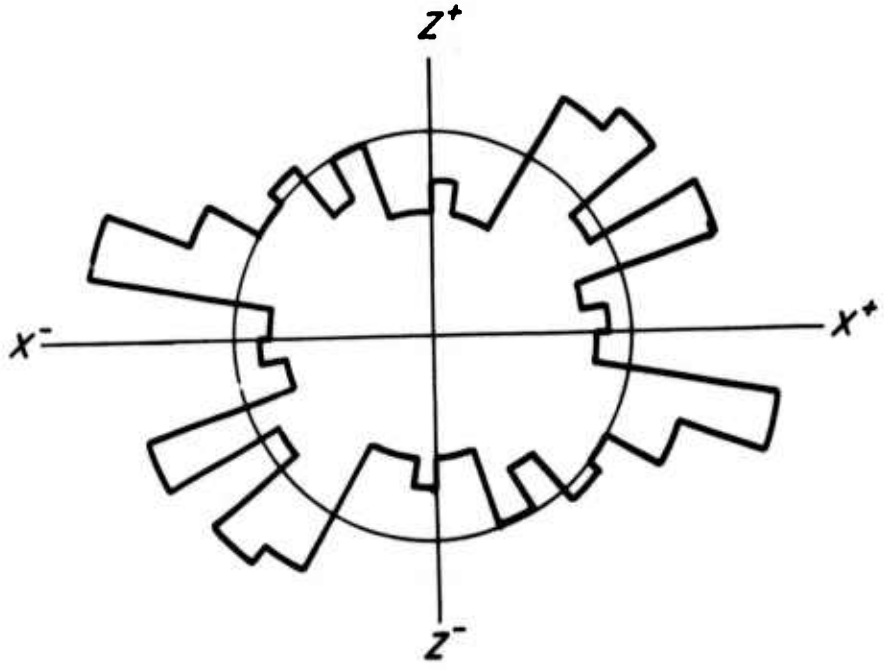

(b) Moist tamped. $L=12.5\%$, $\bar{\theta}=86°$

FIG. 23 ROSE DIAGRAMS OF PARTICLE LONG AXIS ORIENTATIONS FOR SAMPLES OF MONTEREY NO. 0 SAND PREPARED TO 80% RELATIVE DENSITY BY DIFFERENT METHODS

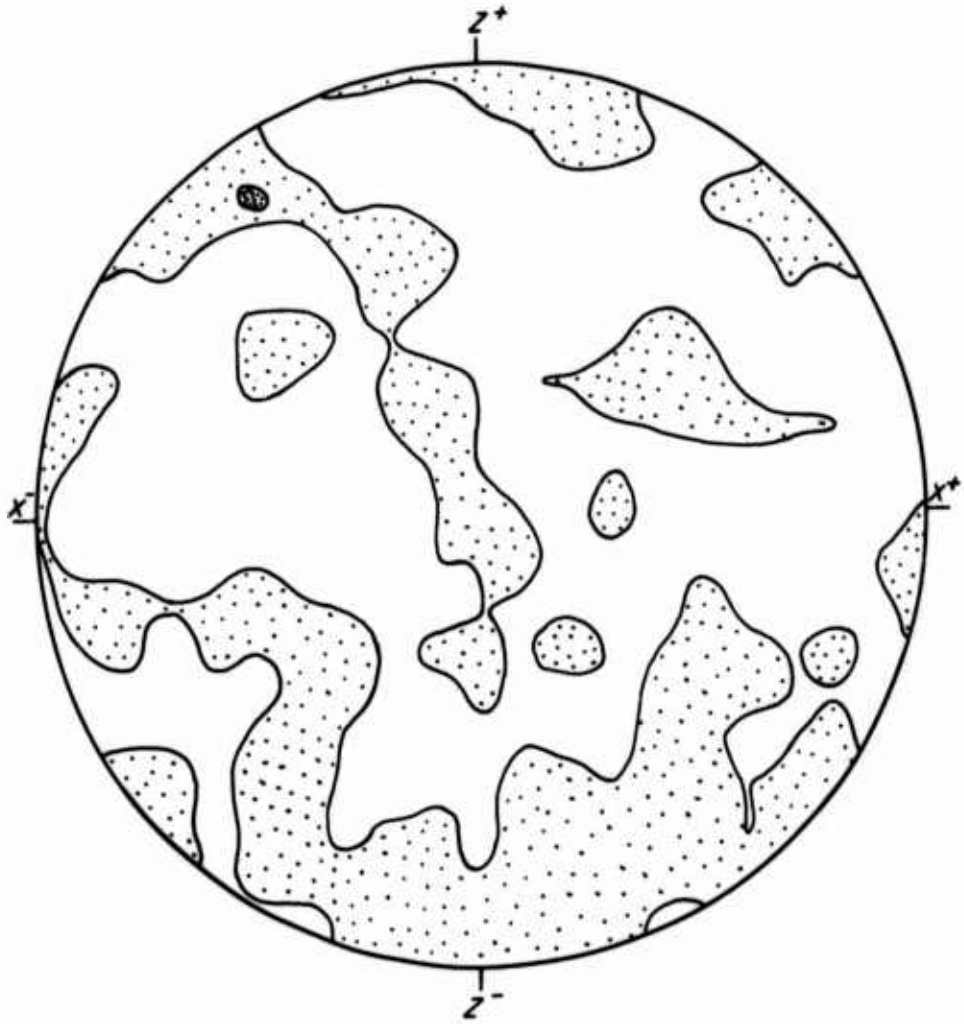

FIG. 24 EQUAL AREA STEREONET SHOWING DISTRIBUTION OF INTERPARTICLE CONTACT NORMALS IN A SAMPLE PREPARED BY PLUVIAL COMPACTION TO A RELATIVE DENSITY OF 50%

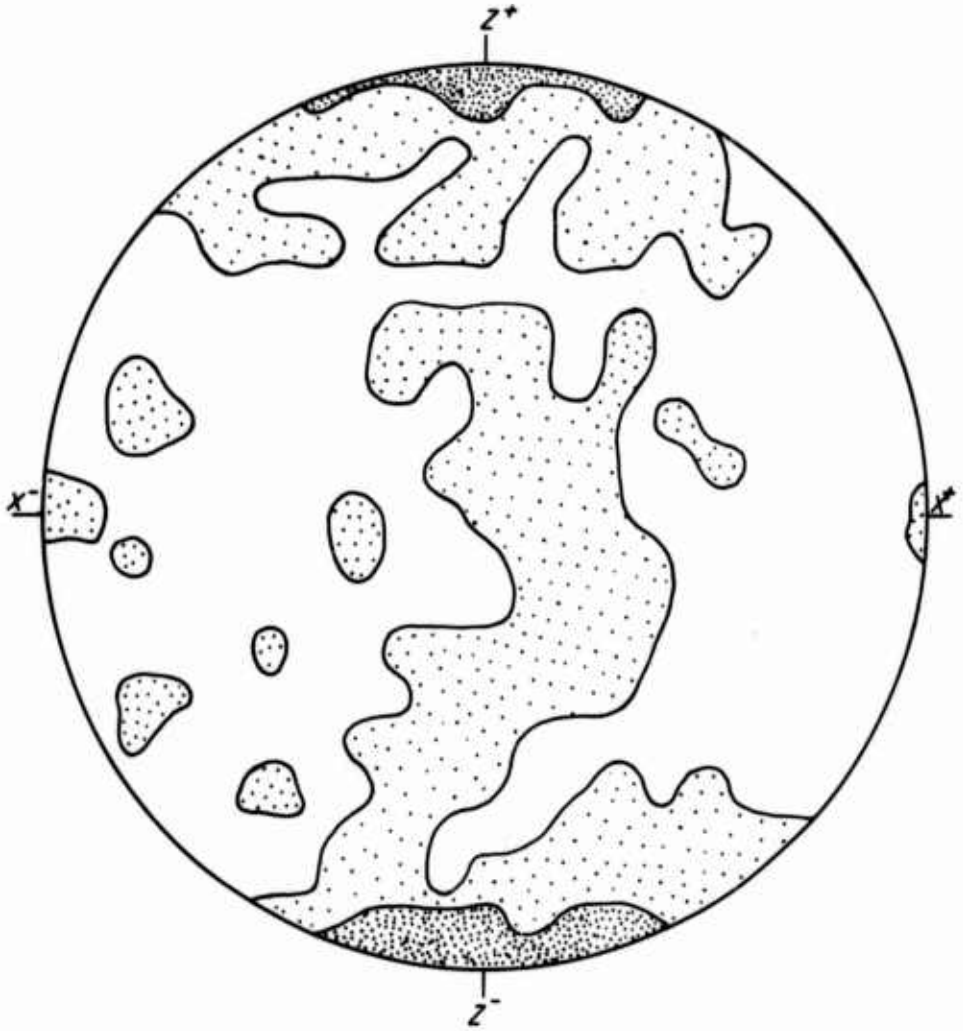

FIG. 25 EQUAL AREA STEREONET SHOWING DISTRIBUTION OF INTERPARTICLE CONTACT NORMALS IN A SAMPLE PREPARED BY MOIST TAMPING TO A RELATIVE DENSITY OF 50%

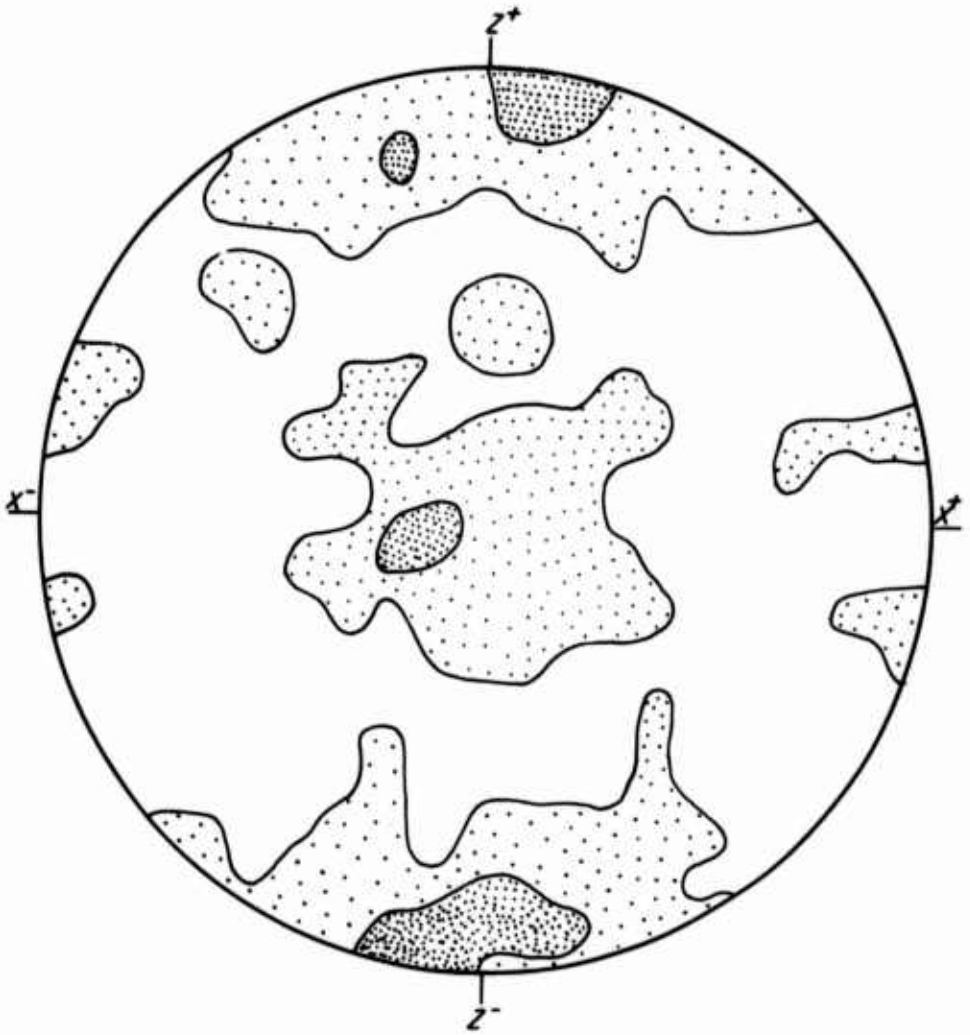

FIG. 26 EQUAL AREA STEREONET SHOWING DISTRIBUTION OF INTERPARTICLE CONTACT NORMALS IN A SAMPLE PREPARED BY MOIST VIBRATION TO A RELATIVE DENSITY OF 50%

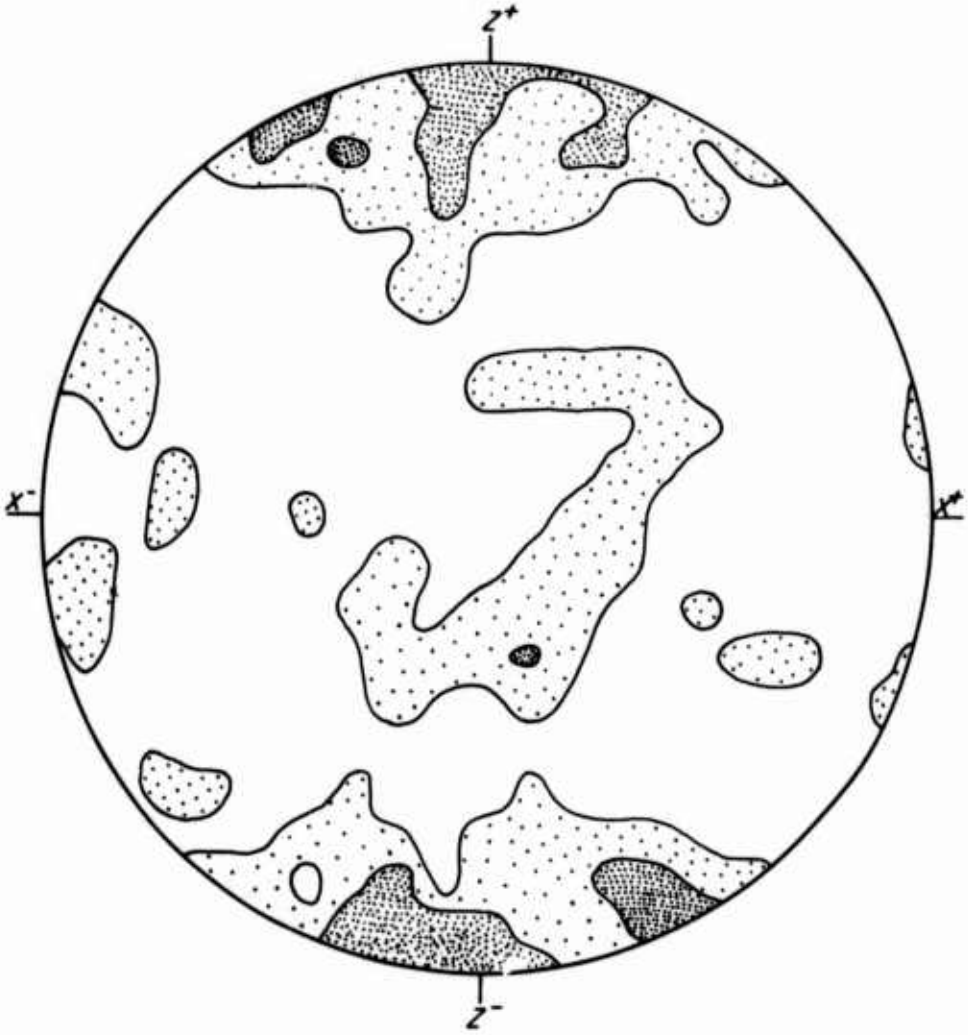

FIG. 27 EQUAL AREA STEREONET SHOWING DISTRIBUTION OF INTERPARTICLE CONTACT NORMALS IN A SAMPLE PREPARED BY PLUVIATION TO A RELATIVE DENSITY OF 80%

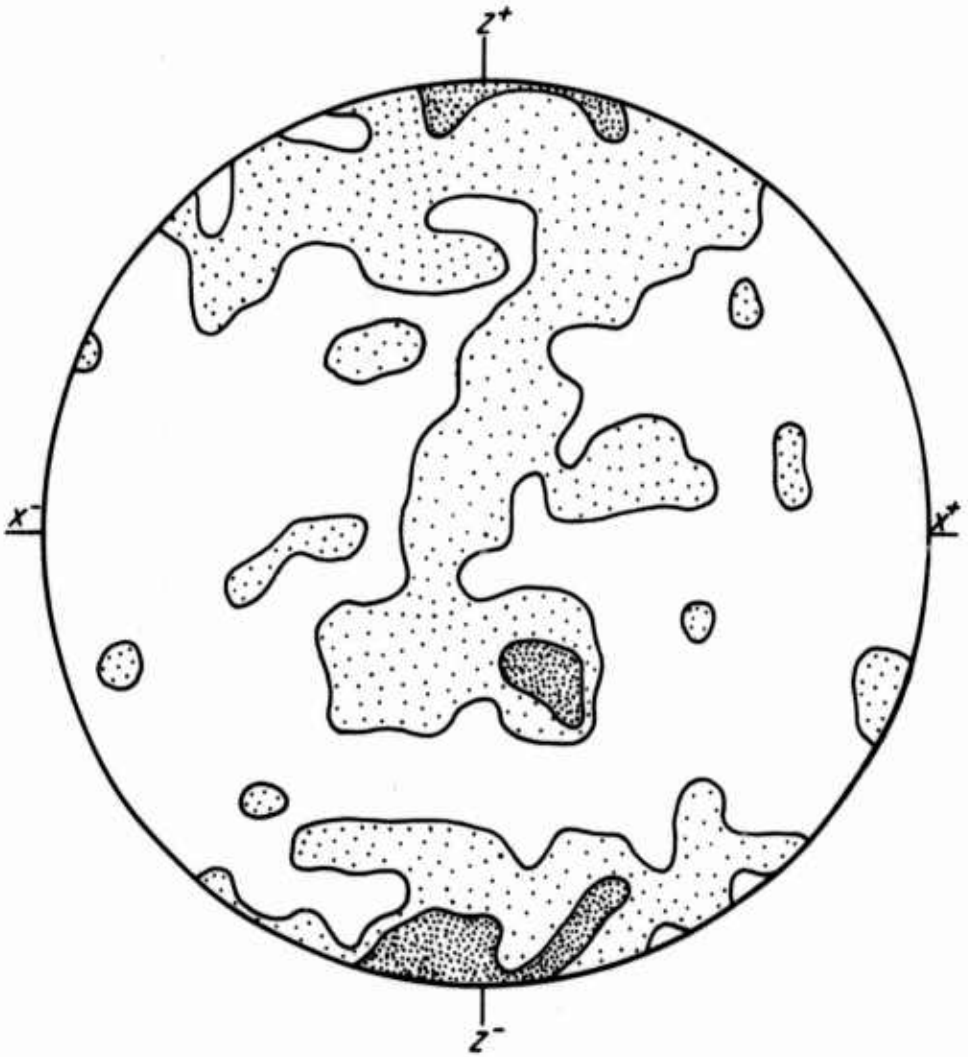

FIG. 28 EQUAL AREA STEREONET SHOWING DISTRIBUTION OF INTERPARTICLE CONTACT NORMALS IN A SAMPLE PREPARED BY MOIST TAMPING TO A RELATIVE DENSITY OF 80%

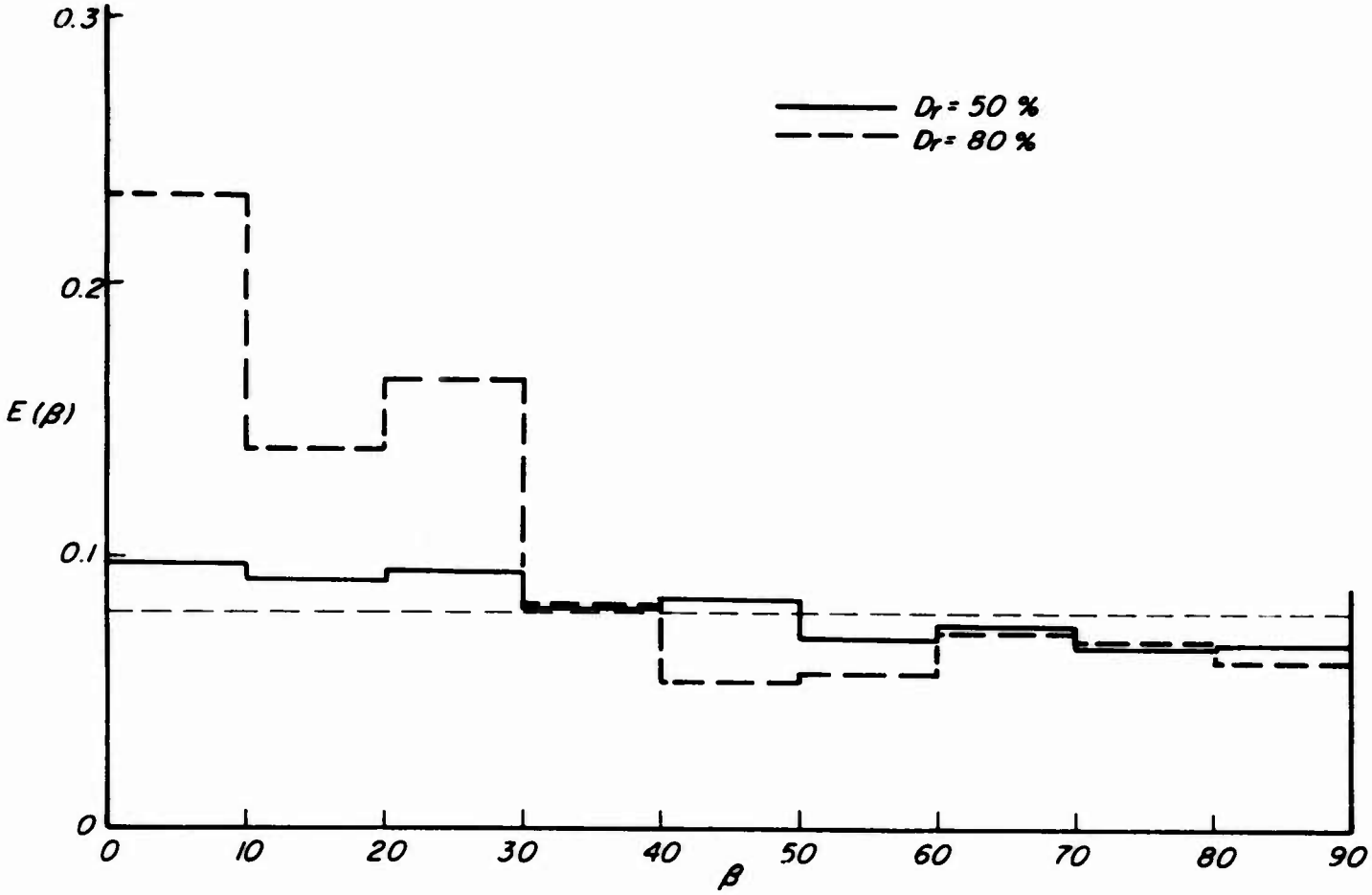

FIG. 29 INTERPARTICLE CONTACT NORMAL DISTRIBUTION FUNCTIONS FOR SAMPLES PREPARED BY PLUVIAL COMPACTION

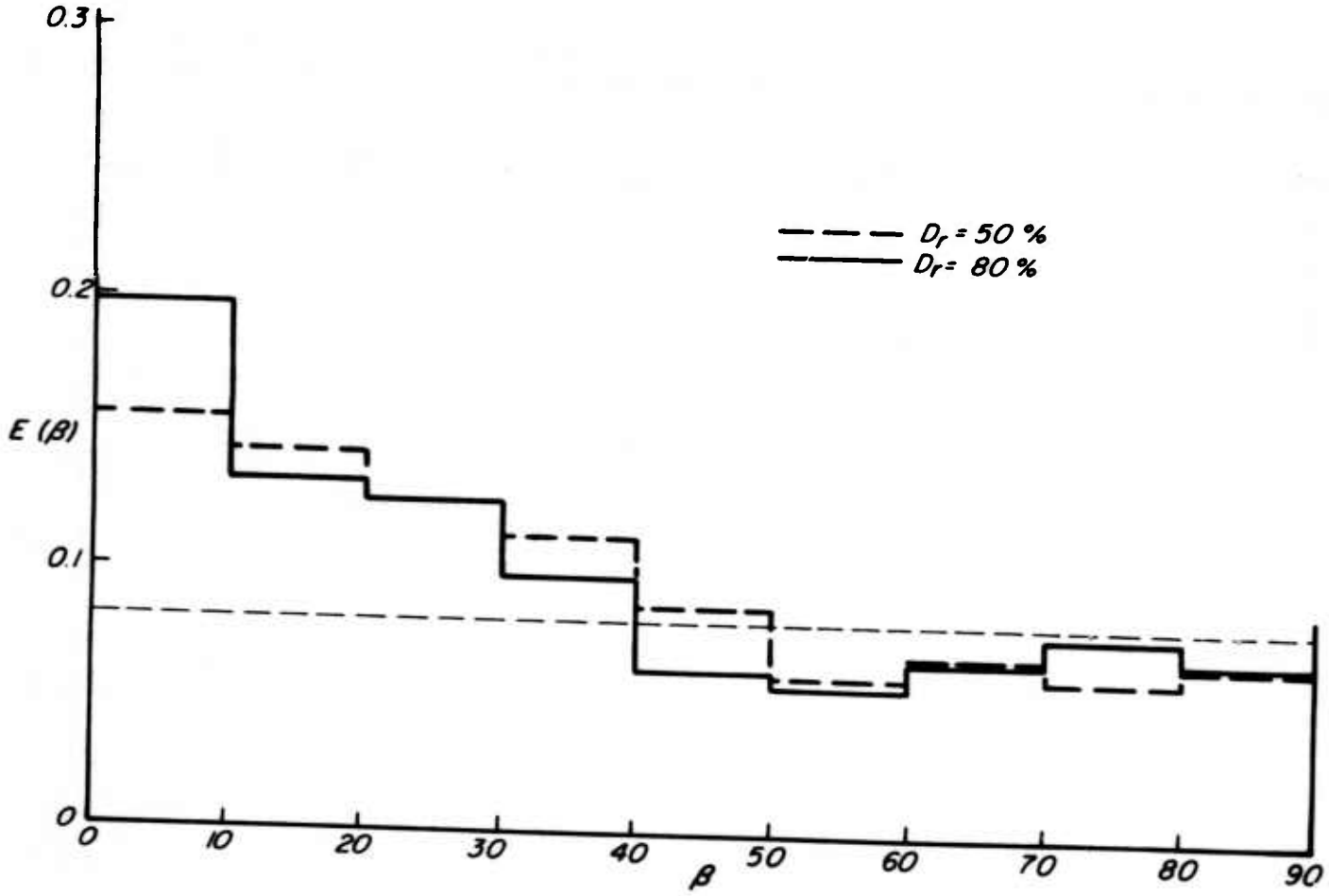

FIG. 30 INTERPARTICLE CONTACT NORMAL DISTRIBUTION FUNCTIONS FOR SAMPLES PREPARED BY MOIST TAMPING

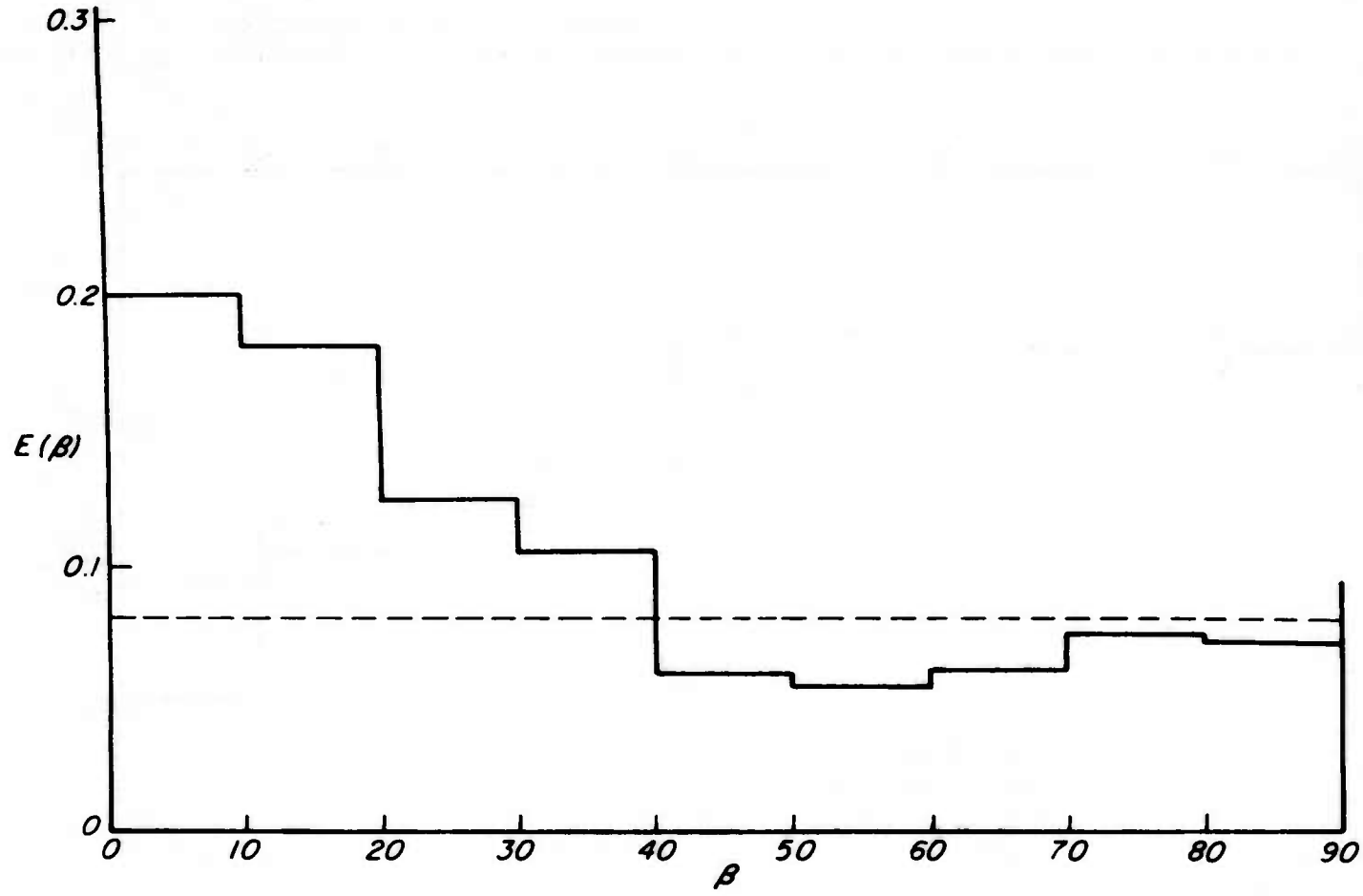

FIG. 31 INTERPARTICLE CONTACT NORMAL DISTRIBUTION FUNCTION FOR SAMPLE PREPARED TO A RELATIVE DENSITY OF 50% BY MOIST VIBRATION

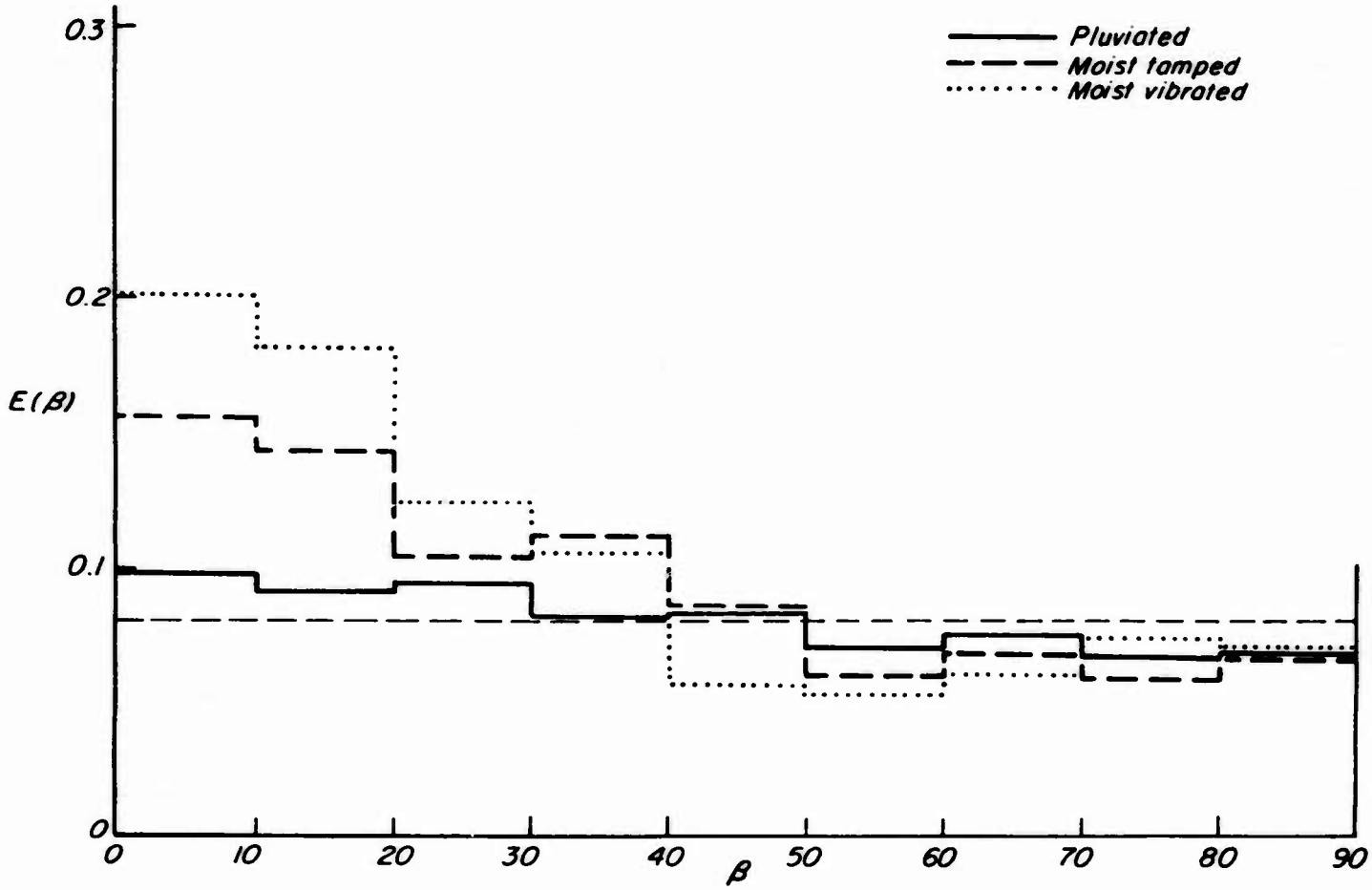

FIG. 32 INTERPARTICLE CONTACT NORMAL DISTRIBUTIONS FOR SAMPLES PREPARED TO A RELATIVE DENSITY OF 50% BY THREE METHODS

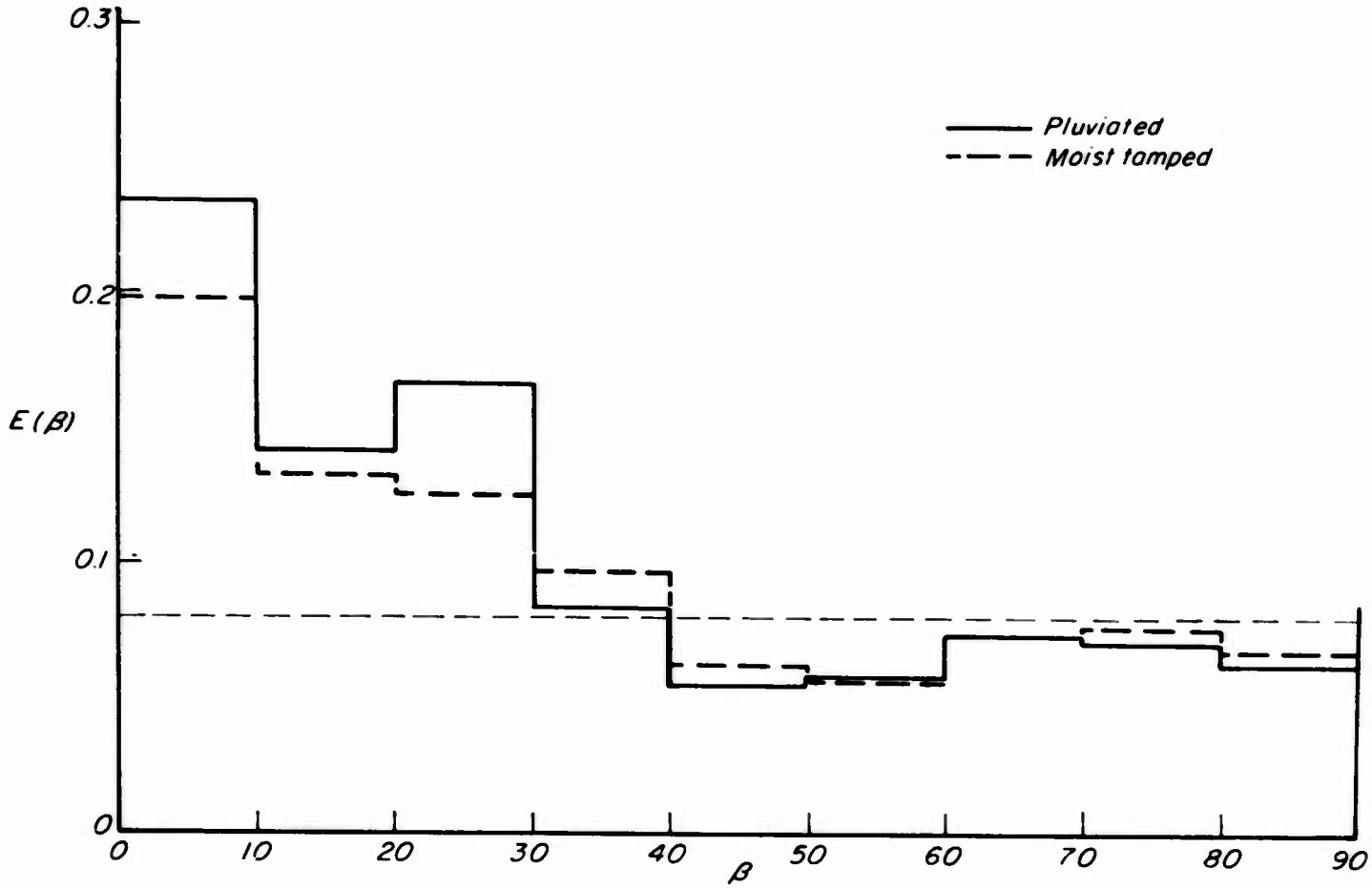

FIG. 33 INTERPARTICLE CONTACT NORMAL DISTRIBUTIONS FOR SAMPLES PREPARED TO A RELATIVE DENSITY OF 80% BY TWO METHODS

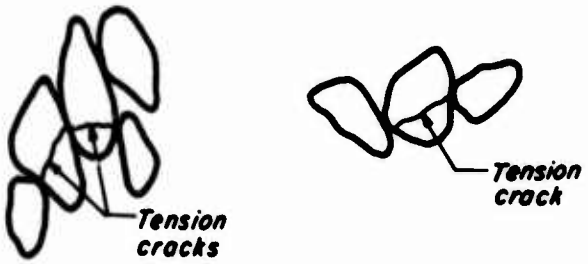

FIG. 34 SCHEMATIC DIAGRAM OF TENSION CRACKS IN GRAINS WITHIN MOIST VIBRATED AND MOIST TAMPED SAMPLES OF MONTEREY NO. 0 SAND

FIG. 35 SCHEMATIC DIAGRAM OF A LARGE PORE AS SEEN IN HORIZONTAL THIN SECTION (~60X MAGNIFICATION)

In accordance with ER 70-2-3, paragraph 6c(1)(b), dated 15 February 1973, a facsimile catalog card in Library of Congress format is reproduced below.

Mitchell, James K

The influences of sand fabric on liquefaction behavior, by James K. Mitchell, John M. Chatoian, [and] Gary C. Carpenter, College of Engineering, University of California, Berkeley, California. Vicksburg, U. S. Army Engineer Waterways Experiment Station, 1976.

viii, 38 p. illus. 27 cm. (U. S. Waterways Experiment Station. Contract report S-76-5)

Prepared for Office, Chief of Engineers, U. S. Army, Washington, D. C., under Contract No. DACA 39-75-M0260 and Military RDTE Program 4A161102AT22.

References: p. 38.

1. Liquefaction (Soils). 2. Sands. 3. Soil fabric. 4. Triaxial shear tests. I. Carpenter, Gary C., joint author. II. Chatoian, John M., joint author. III. California. University. College of Engineering. IV. U. S. Army. Corps of Engineers. (Series: U. S. Waterways Experiment Station, Vicksburg, Miss. Contract report S-76-5)
TA7.W34c no.S-76-5